Light single-gluon hybrid states with various exotic quantum numbers

Wei-Han Tan,[1] Niu Su,[1,2] and Hua-Xing Chen[1,*]
[1]School of Physics, Southeast University, Nanjing 210094, China
[2]Research Center for Nuclear Physics (RCNP), Osaka University, Ibaraki 567-0047, Japan

(Received 16 April 2024; accepted 24 July 2024; published 23 August 2024)

We apply the QCD sum rule method to study the light single-gluon hybrid states with various (exotic) quantum numbers. We construct 24 single-gluon hybrid currents and use 18 of them to calculate the masses of 44 single-gluon hybrid states with the quark-gluon contents $\bar{q}qg$ ($q = u/d$) and $\bar{s}sg$. We concentrate on the hybrid states with the exotic quantum number $J^{PC} = 1^{-+}$, whose masses and widths are calculated to be $M_{|\bar{q}qg;1^-1^{-+}\rangle} = 1.67^{+0.15}_{-0.17}$ GeV, $\Gamma_{|\bar{q}qg;1^-1^{-+}\rangle} = 530^{+540}_{-330}$ MeV, $M_{|\bar{q}qg;0^+1^{-+}\rangle} = 1.67^{+0.15}_{-0.17}$ GeV, $\Gamma_{|\bar{q}qg;0^+1^{-+}\rangle} = 120^{+160}_{-110}$ MeV, $M_{|\bar{s}sg;0^+1^{-+}\rangle} = 1.84^{+0.14}_{-0.15}$ GeV, and $\Gamma_{|\bar{s}sg;0^+1^{-+}\rangle} = 100^{+110}_{-80}$ MeV. Our results support the interpretations of the $\pi_1(1600)$ and $\eta_1(1855)$ as the hybrid states $|\bar{q}qg;1^-1^{-+}\rangle$ and $|\bar{s}sg;0^+1^{-+}\rangle$, respectively. Considering the uncertainties, our results suggest that the $\pi_1(1600)$ and $\eta_1(1855)$ may also be interpreted as the hybrid states $|\bar{q}qg;1^-1^{-+}\rangle$ and $|\bar{q}qg;0^+1^{-+}\rangle$, respectively. To differentiate these two assignments and to verify whether they are hybrid states or not, we propose to examine the $a_1(1260)\pi$ decay channel in future experiments.

DOI: 10.1103/PhysRevD.110.034031

I. INTRODUCTION

A single-gluon hybrid state is composed of one valence quark and one valence antiquark as well as one valence gluon. Especially, the hybrid states with $J^{PC} = 0^{\pm-}/1^{-+}/2^{+-}/3^{-+}/\cdots$ are of particular interest, since these exotic quantum numbers cannot be accessed by the conventional $\bar{q}q$ meson [1–11]. Experimental confirmation of the hybrid state is a direct test of QCD in the low-energy sector. Recently, the BESIII Collaboration performed a partial wave analysis of the $J/\psi \to \gamma\eta\eta'$ decay and observed the $\eta_1(1855)$ in the $\eta\eta'$ mass spectrum with a statistical significance larger than 19σ [12,13]. This state has the exotic quantum number $I^G J^{PC} = 0^+1^{-+}$. Its mass and width were measured to be

$$\eta_1(1855){:}\ M = 1855 \pm 9^{+6}_{-1}\ \mathrm{MeV}/c^2,\quad \Gamma = 188 \pm 18^{+3}_{-8}\ \mathrm{MeV}. \tag{1}$$

Besides the isoscalar state $\eta_1(1855)$, there are three isovector states, $\pi_1(1400)$ [14], $\pi_1(1600)$ [15], and $\pi_1(2015)$ [16], which have the exotic quantum number $I^G J^{PC} = 1^-1^{-+}$. According to PDG, their masses and widths are [1]

$$\pi_1(1400){:}\ M = 1354 \pm 25\ \mathrm{MeV},\quad \Gamma = 330 \pm 35\ \mathrm{MeV}; \tag{2}$$

$$\pi_1(1600){:}\ M = 1661^{+15}_{-11}\ \mathrm{MeV},\quad \Gamma = 240 \pm 50\ \mathrm{MeV}; \tag{3}$$

$$\pi_1(2015){:}\ M = 2014 \pm 20 \pm 16\ \mathrm{MeV},\quad \Gamma = 230 \pm 32 \pm 73\ \mathrm{MeV}. \tag{4}$$

The $\pi_1(1400)$ was observed in the $\eta\pi$ decay channel by several collaborations [14,17–21]. It was also observed in the $\rho\pi$ decay channel by OBELIX [22], but this was not confirmed by COMPASS [23]. The $\pi_1(1600)$ was observed in the $\rho\pi$, $\eta'\pi$, $b_1(1235)\pi$, and $f_1(1285)\pi$ decay channels by several collaborations [15,24–27], while the $\pi_1(2015)$ was observed in the $b_1(1235)\pi$ and $f_1(1285)\pi$ decay channels only in the Brookhaven National Laboratory E852 experiments [16,28]. In recent years, the COMPASS and JPAC Collaborations further examined the $\eta\pi$ and $\eta'\pi$ decay channels [23,29–31], and their results suggest that there is only one exotic π_1 resonance coupling to both the $\eta\pi$ and $\eta'\pi$ channels, while there is no evidence for a second exotic resonance. Its mass and width were determined to be $1564 \pm 24 \pm 86$ and $492 \pm 54 \pm 102$ MeV, respectively [29].

In the past 50 years, there have been a lot of theoretical investigations on the hybrid states, such as the MIT bag model [32–34], flux-tube model [35–38], AdS/QCD model [39,40], lattice QCD [41–45], QCD sum rules [46–51], and constituent gluon model [52–54], etc. However, their nature

[*]Contact author: hxchen@seu.edu.cn

remains elusive, since we still poorly understand the gluon degree of freedom. Experimentally, it is not easy to identify the hybrid states unambiguously, so there is currently no definite experimental evidence on their existence. Theoretically, it is also not easy to define the gluon degree of freedom, and a precise definition of the constituent gluon is still lacking. We refer to Refs. [52–59] for discussions on how to construct glueballs and hybrid states using the constituent gluons.

There have been many theoretical calculations on the masses of the $J^{PC} = 1^{-+}$ hybrid states [60–66]. For examples, their masses extracted from the lattice QCD simulations are about 1.7 [67], 1.8 [68], and 2.0 GeV [69], while their masses extracted from the flux-tube model and the constituent gluon model are about 1.9 GeV [70–72]. The QCD sum rule method has been widely applied to study the $J^{PC} = 1^{-+}$ hybrid states in Refs. [73–79], and this method has also been applied to study the $J^{PC} = 0^{+-}$ and 2^{+-} hybrid states in Refs. [80,81]. We refer to Refs. [82–108] for more theoretical studies. We also refer to our recent review [11] as well as the reviews [2–10] for detailed discussions.

Besides the exotic quantum numbers $J^{PC} = 0^{+-}/1^{-+}/2^{+-}$, the light single-gluon hybrid states with other quantum numbers have not been well studied in the literature. Accordingly, in this paper, we shall systematically investigate the single-gluon hybrid states with various (exotic) quantum numbers through the QCD sum rule method. Especially, we shall concentrate on the hybrid states with the exotic quantum number $J^{PC} = 1^{-+}$ and update the previous calculations on their mass spectrum [76], given that some QCD parameters have been significantly changed in recent years. We shall also update our previous calculations on their decay properties [109–111], with more decay channels taken into account (see the caption of Table III). Assuming their quark-gluon contents to be either $\bar{q}qg$ ($q = u/d$) or $\bar{s}sg$ and their isospin to be either $I = 1$ or $I = 0$, we shall calculate their masses and widths to be

$$
\begin{aligned}
M_{|\bar{q}qg;1^-1^{-+}\rangle} &= 1.67^{+0.15}_{-0.17}\ \text{GeV},\\
\Gamma_{|\bar{q}qg;1^-1^{-+}\rangle} &= 530^{+540}_{-330}\ \text{MeV},\\
M_{|\bar{q}qg;0^+1^{-+}\rangle} &= 1.67^{+0.15}_{-0.17}\ \text{GeV},\\
\Gamma_{|\bar{q}qg;0^+1^{-+}\rangle} &= 120^{+160}_{-110}\ \text{MeV},\\
M_{|\bar{s}sg;0^+1^{-+}\rangle} &= 1.84^{+0.14}_{-0.15}\ \text{GeV},\\
\Gamma_{|\bar{s}sg;0^+1^{-+}\rangle} &= 100^{+110}_{-80}\ \text{MeV}.
\end{aligned}
$$

This paper is organized as follows. In Sec. II, we construct 24 single-gluon hybrid currents with various (exotic) quantum numbers. In Sec. III, we use 18 of them to perform QCD sum rule analyses and calculate masses of 44 single-gluon hybrid states with the quark-gluon contents $\bar{q}qg$ ($q = u/d$) and $\bar{s}sg$. Based on these results, we systematically study the decay properties of the $J^{PC} = 1^{-+}$ hybrid states in Sec. IV. The obtained results are summarized in Sec. V.

II. SINGLE-GLUON HYBRID CURRENTS

In this section, we systematically construct the single-gluon hybrid currents using the light quark field $q_a(x)$ and its dual field $\bar{q}_a(x)$ as well as the gluon field strength tensor $G^n_{\mu\nu}(x)$ and its dual field $\tilde{G}^n_{\mu\nu} = G^{n,\rho\sigma} \times \epsilon_{\mu\nu\rho\sigma}/2$, with $a = 1...3$ and $n = 1...8$ the color indices and $\mu...\sigma$ the Lorentz indices. Generally speaking, we can construct the single-gluon hybrid currents by combining the color-octet quark-antiquark fields

$$
\begin{gathered}
\bar{q}_a \lambda_n^{ab} \gamma_5 q_b, \quad \bar{q}_a \lambda_n^{ab} q_b,\\
\bar{q}_a \lambda_n^{ab} \gamma_\mu q_b, \quad \bar{q}_a \lambda_n^{ab} \gamma_\mu \gamma_5 q_b,\\
\bar{q}_a \lambda_n^{ab} \sigma_{\mu\nu} q_b
\end{gathered}
\tag{5}
$$

and the color-octet gluon fields

$$
G_n^{\alpha\beta}, \qquad \tilde{G}_n^{\alpha\beta}, \tag{6}
$$

together with some Lorentz coefficients $\Gamma^{\mu\nu...\alpha\beta}$.

As summarized in Fig. 1, there are altogether 24 single-gluon hybrid currents, denoted as $J_{J^{PC}}^{\cdots}/\tilde{J}_{J^{PC}}^{\cdots}$ with J the total spin:

$$J_{1^{--}}^{\alpha\beta} = \bar{q}_a \lambda_n^{ab} \gamma_5 q_b g_s G_n^{\alpha\beta}, \tag{7}$$

$$\tilde{J}_{1^{+-}}^{\alpha\beta} = \bar{q}_a \lambda_n^{ab} \gamma_5 q_b g_s \tilde{G}_n^{\alpha\beta}, \tag{8}$$

$$J_{1^{+-}}^{\alpha\beta} = \bar{q}_a \lambda_n^{ab} q_b g_s G_n^{\alpha\beta}, \tag{9}$$

$$\tilde{J}_{1^{--}}^{\alpha\beta} = \bar{q}_a \lambda_n^{ab} q_b g_s \tilde{G}_n^{\alpha\beta}, \tag{10}$$

$$J_{1^{-+}}^{\mu} = \bar{q}_a \lambda_n^{ab} \gamma_\beta q_b g_s G_n^{\mu\beta}, \tag{11}$$

$$\tilde{J}_{1^{++}}^{\mu} = \bar{q}_a \lambda_n^{ab} \gamma_\beta q_b g_s \tilde{G}_n^{\mu\beta}, \tag{12}$$

$$J_{1^{+-}}^{\mu} = \bar{q}_a \lambda_n^{ab} \gamma_\beta \gamma_5 q_b g_s G_n^{\mu\beta}, \tag{13}$$

$$\tilde{J}_{1^{--}}^{\mu} = \bar{q}_a \lambda_n^{ab} \gamma_\beta \gamma_5 q_b g_s \tilde{G}_n^{\mu\beta}, \tag{14}$$

$$J_{2^{-+}}^{\mu,\alpha\beta} = \bar{q}_a \lambda_n^{ab} \gamma^\mu q_b g_s G_n^{\alpha\beta}, \tag{15}$$

$$\tilde{J}_{2^{++}}^{\mu,\alpha\beta} = \bar{q}_a \lambda_n^{ab} \gamma^\mu q_b g_s \tilde{G}_n^{\alpha\beta}, \tag{16}$$

$$J_{2^{+-}}^{\mu,\alpha\beta} = \bar{q}_a \lambda_n^{ab} \gamma^\mu \gamma_5 q_b g_s G_n^{\alpha\beta}, \tag{17}$$

$$\tilde{J}_{2^{--}}^{\mu,\alpha\beta} = \bar{q}_a \lambda_n^{ab} \gamma^\mu \gamma_5 q_b g_s \tilde{G}_n^{\alpha\beta}, \tag{18}$$

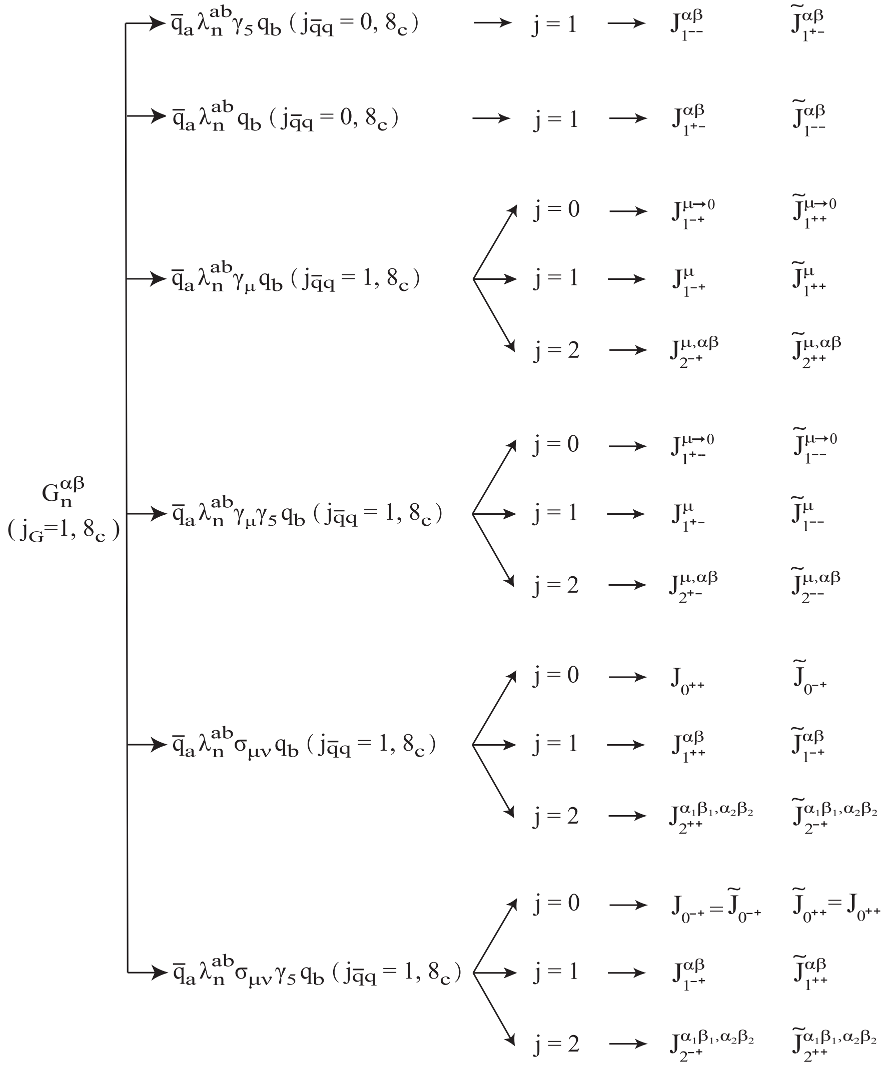

FIG. 1. Categorization of the single-gluon hybrid currents.

$$J_{0^{++}} = \bar{q}_a \lambda_n^{ab} \sigma_{\mu\nu} q_b g_s G_n^{\mu\nu}, \tag{19}$$

$$\tilde{J}_{0^{-+}} = \bar{q}_a \lambda_n^{ab} \sigma_{\mu\nu} q_b g_s \tilde{G}_n^{\mu\nu}, \tag{20}$$

$$J_{0^{-+}} = \bar{q}_a \lambda_n^{ab} \sigma_{\mu\nu} \gamma_5 q_b g_s G_n^{\mu\nu}, \tag{21}$$

$$\tilde{J}_{0^{++}} = \bar{q}_a \lambda_n^{ab} \sigma_{\mu\nu} \gamma_5 q_b g_s \tilde{G}_n^{\mu\nu}, \tag{22}$$

$$J_{1^{++}}^{\alpha\beta} = \mathcal{A}[\bar{q}_a \lambda_n^{ab} \sigma^{\alpha\mu} q_b g_s G_{n,\mu}^{\beta}], \tag{23}$$

$$\tilde{J}_{1^{-+}}^{\alpha\beta} = \mathcal{A}[\bar{q}_a \lambda_n^{ab} \sigma^{\alpha\mu} q_b g_s \tilde{G}_{n,\mu}^{\beta}], \tag{24}$$

$$J_{1^{-+}}^{\alpha\beta} = \mathcal{A}[\bar{q}_a \lambda_n^{ab} \sigma^{\alpha\mu} \gamma_5 q_b g_s G_{n,\mu}^{\beta}], \tag{25}$$

$$\tilde{J}_{1^{++}}^{\alpha\beta} = \mathcal{A}[\bar{q}_a \lambda_n^{ab} \sigma^{\alpha\mu} \gamma_5 q_b g_s \tilde{G}_{n,\mu}^{\beta}], \tag{26}$$

$$J_{2^{++}}^{\alpha_1\beta_1,\alpha_2\beta_2} = \mathcal{S}[\bar{q}_a \lambda_n^{ab} \sigma^{\alpha_1\beta_1} q_b g_s G_n^{\alpha_2\beta_2}], \tag{27}$$

$$\tilde{J}_{2^{-+}}^{\alpha_1\beta_1,\alpha_2\beta_2} = \mathcal{S}[\bar{q}_a \lambda_n^{ab} \sigma^{\alpha_1\beta_1} q_b g_s \tilde{G}_n^{\alpha_2\beta_2}], \tag{28}$$

$$J_{2^{-+}}^{\alpha_1\beta_1,\alpha_2\beta_2} = \mathcal{S}[\bar{q}_a \lambda_n^{ab} \sigma^{\alpha_1\beta_1} \gamma_5 q_b g_s G_n^{\alpha_2\beta_2}], \tag{29}$$

$$\tilde{J}_{2^{++}}^{\alpha_1\beta_1,\alpha_2\beta_2} = \mathcal{S}[\bar{q}_a \lambda_n^{ab} \sigma^{\alpha_1\beta_1} \gamma_5 q_b g_s \tilde{G}_n^{\alpha_2\beta_2}]. \tag{30}$$

Especially, we shall concentrate on the fifth current $J_{1^{-+}}^{\mu}$ with the exotic quantum number $J^{PC} = 1^{-+}$, while this current also contains the $J^{PC} = 0^{++}$ component, so we need to separate the $J^{PC} = 1^{-+}$ and 0^{++} components in the calculations, as discussed below. In the above expressions, $\{\alpha\beta\}/\{\alpha_1\beta_1\}/\{\alpha_2\beta_2\}$ are antisymmetric Lorentz pairs. The four currents $J_{2^{-+}}^{\mu,\alpha\beta}$, $\tilde{J}_{2^{++}}^{\mu,\alpha\beta}$, $J_{2^{+-}}^{\mu,\alpha\beta}$, and $\tilde{J}_{2^{--}}^{\mu,\alpha\beta}$ all contain three Lorentz indices with the mixed symmetry, so their spin-2 components cannot be easily extracted. We shall not investigate these four currents in the present study, and we refer to Ref. [81] for detailed discussions. The symbol

$\mathcal{A}[\cdots]$ represents antisymmetrization in the set $\{\alpha\beta\}$, which can be done by multiplying the projection operator

$$\Gamma_{\alpha'\beta';\alpha\beta} = g_{\alpha'\alpha}g_{\beta'\beta} - g_{\beta'\alpha}g_{\alpha'\beta}. \tag{31}$$

The symbol $\mathcal{S}[\cdots]$ represents symmetrization and subtracting trace terms in the two sets $\{\alpha_1\alpha_2\}$ and $\{\beta_1\beta_2\}$ simultaneously. In the present study, we need to investigate only its leading spin-2 component, which can be done by multiplying the projection operator

$$\begin{aligned}
&\Gamma'_{\alpha'_1\beta'_1,\alpha'_2\beta'_2;\alpha_1\beta_1,\alpha_2\beta_2}\\
&= (g_{\alpha'_1\alpha_1}g_{\beta'_1\beta_1} - g_{\beta'_1\alpha_1}g_{\alpha'_1\beta_1})(g_{\alpha'_2\alpha_2}g_{\beta'_2\beta_2} - g_{\beta'_2\alpha_2}g_{\alpha'_2\beta_2})\\
&\quad + (g_{\alpha'_1\alpha_2}g_{\beta'_1\beta_1} - g_{\beta'_1\alpha_2}g_{\alpha'_1\beta_1})(g_{\alpha'_2\alpha_1}g_{\beta'_2\beta_2} - g_{\beta'_2\alpha_1}g_{\alpha'_2\beta_2})\\
&\quad + (g_{\alpha'_1\alpha_1}g_{\beta'_1\beta_2} - g_{\beta'_1\alpha_1}g_{\alpha'_1\beta_2})(g_{\alpha'_2\alpha_2}g_{\beta'_2\beta_1} - g_{\beta'_2\alpha_2}g_{\alpha'_2\beta_1})\\
&\quad + (g_{\alpha'_1\alpha_2}g_{\beta'_1\beta_2} - g_{\beta'_1\alpha_2}g_{\alpha'_1\beta_2})(g_{\alpha'_2\alpha_1}g_{\beta'_2\beta_1} - g_{\beta'_2\alpha_1}g_{\alpha'_2\beta_1})\\
&\quad + \cdots,
\end{aligned} \tag{32}$$

where $\cdots$ contains the irrelevant terms.

Before performing QCD sum rule analyses, we separately discuss the Lorentz structures of the above single-gluon hybrid currents as follows.

(i) Because of the formula $\sigma_{\mu\nu}\gamma_5 = \epsilon_{\mu\nu\rho\sigma}\sigma^{\rho\sigma} \times i/2$, the two currents $J_{0^{++}}$ and $\tilde{J}_{0^{++}}$ are equivalent, and the other two currents $J_{0^{-+}}$ and $\tilde{J}_{0^{-+}}$ are also equivalent. Hence, we shall study only the currents $J_{0^{++}}$ and $J_{0^{-+}}$.

(ii) The current $J^{\alpha\beta}_{1^{--}}$, with two antisymmetric Lorentz indices $\{\alpha\beta\}$, contains both the $J^{PC} = 1^{--}$ and 1^{+-} components, so it couples to both the $J^{PC} = 1^{--}$ and 1^{+-} states through

$$\langle 0|J^{\alpha\beta}_{1^{--}}|X_{1^{--}}\rangle = i f_{1^{--}}\epsilon^{\alpha\beta\mu\nu}\epsilon_\mu q_\nu, \tag{33}$$

$$\langle 0|J^{\alpha\beta}_{1^{--}}|\tilde{X}_{1^{+-}}\rangle = i\tilde{f}_{1^{+-}}(q^\alpha\epsilon^\beta - q^\beta\epsilon^\alpha), \tag{34}$$

where $f_{1^{--}}$ and $\tilde{f}_{1^{+-}}$ are two decay constants. Given the Lorentz structures of Eqs. (33) and (34) to be totally different, we can clearly separate the two states $X_{1^{--}}$ and $\tilde{X}_{1^{+-}}$ at the hadron level; i.e., we can isolate $X_{1^{--}}$ by investigating the two-point correlation function containing

$$\begin{aligned}
&\langle 0|J^{\alpha\beta}_{1^{--}}|X_{1^{--}}\rangle\langle X_{1^{--}}|J^{\alpha'\beta'\dagger}_{1^{--}}|0\rangle\\
&= f^2_{1^{--}}\epsilon^{\alpha\beta\mu\nu}\epsilon_\mu q_\nu \epsilon^{\alpha'\beta'\mu'\nu'}\epsilon^*_{\mu'}q_{\nu'}\\
&= -f^2_{1^{--}}q^2(g^{\alpha\alpha'}g^{\beta\beta'} - g^{\alpha\beta'}g^{\beta\alpha'}) + \cdots,
\end{aligned} \tag{35}$$

while the correlation function of $\tilde{X}_{1^{+-}}$ does not contain the above coefficient. It is not so easy to isolate $\tilde{X}_{1^{+-}}$ from $J^{\alpha\beta}_{1^{--}}$, but, instead, we can study the dual current $\tilde{J}^{\alpha\beta}_{1^{+-}}$ that couples to $X_{1^{--}}$ and $\tilde{X}_{1^{+-}}$ in the opposite ways. According to the above analysis, we shall study the single-gluon hybrid currents $J^{\alpha\beta}_{1^{--}}/\tilde{J}^{\alpha\beta}_{1^{+-}}/J^{\alpha\beta}_{1^{+-}}/\tilde{J}^{\alpha\beta}_{1^{--}}/J^{\alpha\beta}_{1^{++}}/\tilde{J}^{\alpha\beta}_{1^{-+}}/J^{\alpha\beta}_{1^{-+}}/\tilde{J}^{\alpha\beta}_{1^{++}}$ to investigate the single-gluon hybrid states of $J^{PC} = 1^{--}/1^{+-}/1^{+-}/1^{--}/1^{++}/1^{-+}/1^{-+}/1^{++}$, respectively.

(iii) The four currents $J^{\alpha_1\beta_1,\alpha_2\beta_2}_{2^{++}}$, $\tilde{J}^{\alpha_1\beta_1,\alpha_2\beta_2}_{2^{-+}}$, $J^{\alpha_1\beta_1,\alpha_2\beta_2}_{2^{-+}}$, and $\tilde{J}^{\alpha_1\beta_1,\alpha_2\beta_2}_{2^{++}}$ all contain various J^{PC} components and so couple to many states. We shall investigate only the four $J = 2$ states of $J^{PC} = 2^{++}/2^{-+}/2^{-+}/2^{++}$ by calculating the highest-order correlation functions, e.g.,

$$\begin{aligned}
&\Pi^{\alpha_1\beta_1,\alpha_2\beta_2;\alpha'_1\beta'_1,\alpha'_2\beta'_2}_{2^{++}}(q^2)\\
&= i\int d^4x e^{iqx}\langle 0|\mathbf{T}[J^{\alpha_1\beta_1,\alpha_2\beta_2}_{2^{++}}(x)J^{\alpha'_1\beta'_1,\alpha'_2\beta'_2\dagger}_{2^{++}}(0)]|0\rangle\\
&= \mathcal{S}'[g^{\alpha_1\alpha'_1}g^{\beta_1\beta'_1}g^{\alpha_2\alpha'_2}g^{\beta_2\beta'_2}]\Pi_{2^{++}}(q^2) + \cdots,
\end{aligned} \tag{36}$$

where $\mathcal{S}'[\cdots]$ represents symmetrization and subtracting trace terms in the four sets $\{\alpha_1\alpha_2\}$, $\{\beta_1\beta_2\}$, $\{\alpha'_1\alpha'_2\}$, and $\{\beta'_1\beta'_2\}$ simultaneously. The correlation function $\Pi_{2^{++}}(q^2)$ is contributed only by the $J^{PC} = 2^{++}$ component, while $\cdots$ contains the contributions from all the J^{PC} components coupling to $J^{\alpha_1\beta_1,\alpha_2\beta_2}_{2^{++}}$. However, we do not know the explicit expression of the rearrangement $\mathcal{S}'[\cdots]$, so we are not able to calculate the decay constants of these four currents.

(iv) The current $J^\mu_{1^{-+}}$ contains both the $J^{PC} = 1^{-+}$ and 0^{++} components, so it couples to both the $J^{PC} = 1^{+-}$ and 0^{++} states through

$$\langle 0|J^\mu_{1^{-+}}|X_{1^{-+}}\rangle = \epsilon^\mu f_{1^{-+}}, \tag{37}$$

$$\langle 0|J^\mu_{1^{-+}}|X_{0^{++}}\rangle = q^\mu f_{0^{++}}, \tag{38}$$

where $f_{1^{-+}}$ and $f_{0^{++}}$ are two decay constants. We can clearly separate the two states $X_{1^{-+}}$ and $X_{0^{++}}$ at the hadron level by calculating both $\Pi_{1^{-+}}(q^2)$ and $\Pi_{0^{++}}(q^2)$ of the two-point correlation function

$$\begin{aligned}
&\Pi^{\mu\nu}_{1^{-+}}(q^2)\\
&\equiv i\int d^4x e^{iqx}\langle 0|\mathbf{T}[J^\mu_{1^{-+}}(x)J^{\nu\dagger}_{1^{-+}}(0)]|0\rangle\\
&= (g^{\mu\nu} - q^\mu q^\nu/q^2)\Pi_{1^{-+}}(q^2) + (q^\mu q^\nu/q^2)\Pi_{0^{++}}(q^2).
\end{aligned} \tag{39}$$

Similarly, we shall study the single-gluon hybrid currents $\tilde{J}^\mu_{1^{++}}/J^\mu_{1^{+-}}/\tilde{J}^\mu_{1^{--}}$ to investigate the single-gluon hybrid states of both $J^{PC} = 1^{++}/1^{+-}/1^{--}$ and $J^{PC} = 0^{-+}/0^{--}/0^{+-}$.

III. QCD SUM RULE ANALYSES

In this section, we use the single-gluon hybrid currents given in Eqs. (7)–(14) and (19)–(30) to perform QCD sum rule analyses. We use the current $J^{\mu}_{1^{-+}}$ given in Eq. (11) as an example. Based on Eqs. (37) and (39), we study its two-point correlation function

$$\Pi^{\mu\nu}_{1^{-+}}(q^2) = i\int d^4x e^{iqx}\langle 0|\mathbf{T}[J^{\mu}_{1^{-+}}(x)J^{\nu\dagger}_{1^{-+}}(0)]|0\rangle = (g^{\mu\nu} - q^\mu q^\nu/q^2)\Pi_{1^{-+}}(q^2) + \cdots, \quad (40)$$

at both the hadron and quark-gluon levels, where $\Pi_{1^{-+}}(q^2)$ is contributed by the $J^{PC} = 1^{-+}$ state $X_{1^{-+}}$ and $\cdots$ is contributed by the $J^{PC} = 0^{++}$ state $X_{0^{++}}$.

We use the dispersion relation to express $\Pi_{1^{-+}}(q^2)$ as

$$\Pi_{1^{-+}}(q^2) = \int_{s_<}^{\infty} \frac{\rho_{1^{-+}}(s)}{s - q^2 - i\varepsilon} ds, \quad (41)$$

where $\rho_{1^{-+}}(s) \equiv \mathrm{Im}\Pi_{1^{-+}}(s)/\pi$ is the spectral density and $s_< = 4m_q^2$ is the physical threshold.

At the hadron level, we parametrize $\rho^{\mathrm{phen}}_{1^{-+}}(s)$ as one-pole dominance for the state $X_{1^{-+}}$ together with a continuum contribution:

$$\rho^{\mathrm{phen}}_{1^{-+}}(s) \times (g^{\mu\nu} - q^\mu q^\nu/q^2) \equiv \sum_n \delta(s - M_n^2)\langle 0|J^{\mu}_{1^{-+}}|n\rangle\langle n|J^{\nu\dagger}_{1^{-+}}|0\rangle = f^2_{1^{-+}}\delta(s - M^2_{1^{-+}}) \times (g^{\mu\nu} - q^\mu q^\nu/q^2) + \text{continuum}. \quad (42)$$

At the quark-gluon level, we calculate $\rho^{\mathrm{OPE}}_{1^{-+}}(s)$ through the method of operator product expansion (OPE). After performing the Borel transformation at both the hadron and quark-gluon levels, we use $\rho^{\mathrm{OPE}}_{1^{-+}}(s)$ above the threshold value s_0 to approximate the continuum and derive the sum rule equation

$$\Pi_{1^{-+}}(s_0, M_B^2) \equiv f^2_{1^{-+}} e^{-M^2_{1^{-+}}/M_B^2} = \int_{s_<}^{s_0} e^{-s/M_B^2}\rho^{\mathrm{OPE}}_{1^{-+}}(s) ds, \quad (43)$$

which can be used to further derive

$$M^2_{1^{-+}}(s_0, M_B) = \frac{\int_{s_<}^{s_0} e^{-s/M_B^2} s \rho^{\mathrm{OPE}}_{1^{-+}}(s) ds}{\int_{s_<}^{s_0} e^{-s/M_B^2}\rho^{\mathrm{OPE}}_{1^{-+}}(s) ds}, \quad (44)$$

$$f^2_{1^{-+}}(s_0, M_B) = \Pi_{1^{-+}}(s_0, M_B^2) \times e^{M^2_{1^{-+}}/M_B^2}. \quad (45)$$

In the present study, we have considered the Feynman diagrams depicted in Fig. 2 and calculated $\rho_{\mathrm{OPE}}(s)$ up to the dimension-eight condensates. The gluon field strength tensor $G^n_{\mu\nu}$ is defined as

$$G^n_{\mu\nu} = \partial_\mu A^n_\nu - \partial_\nu A^n_\mu + g_s f^{npq} A_{p,\mu} A_{q,\nu}, \quad (46)$$

which can be separated into the former two terms (represented by the single-gluon line) and the third term [represented by the double-gluon line with a red vertex; e.g., see the diagram depicted in Fig. 2(c2)]. In the calculations, we have considered the perturbative term, the quark condensates, the quark-gluon mixed condensates, the two-gluon condensate, the three-gluon condensate, and their combinations. We have taken into account all the diagrams proportional to $\alpha_s \times g_s^0$ and $\alpha_s \times g_s^1$, but we have taken into account only three diagrams proportional to $\alpha_s \times g_s^2$. We summarize the obtained OPE spectral densities in the Appendix. Especially, the one extracted from the current $J^{\mu}_{1^{-+}}$ with the quark-gluon content $\bar{s}sg$ is

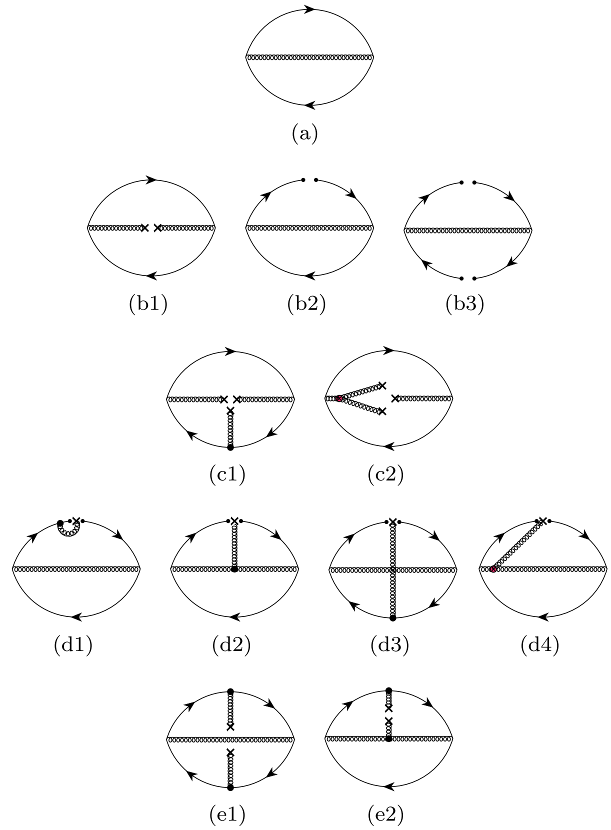

FIG. 2. Feynman diagrams for the single-gluon hybrid state: (a) and (b) are proportional to $\alpha_s \times g_s^0$; (c) and (d) are proportional to $\alpha_s \times g_s^1$; (e) are proportional to $\alpha_s \times g_s^2$.

$$\Pi^{\mu}_{1^{-+}}(M_B^2, s_0) = \int_{4m_s^2}^{s_0}\left(\frac{s^3\alpha_s}{60\pi^3} - \frac{m_s^2 s^2 \alpha_s}{3\pi^3} + s\left(\frac{\langle\alpha_s GG\rangle}{36\pi^2} + \frac{13\langle\alpha_s GG\rangle\alpha_s}{432\pi^3} + \frac{8m_s\langle\bar{s}s\rangle\alpha_s}{9\pi}\right) + \frac{\langle g_s^3 G^3\rangle}{32\pi^2} - \frac{3\langle\alpha_s GG\rangle m_s^2\alpha_s}{64\pi^3} - \frac{3m_s\langle g_s\bar{s}\sigma Gs\rangle\alpha_s}{4\pi}\right) \times e^{-s/M_B^2} ds + \left(\frac{\langle\alpha_s GG\rangle^2}{3456\pi^2} - \frac{\langle g_s^3 G^3\rangle m_s^2}{16\pi^2} - \frac{2}{9}\langle\alpha_s GG\rangle m_s\langle\bar{s}s\rangle + \frac{11\pi\langle\bar{s}s\rangle\langle g_s\bar{s}\sigma Gs\rangle\alpha_s}{9}\right). \quad (47)$$

The one with the quark-gluon content $\bar{q}qg$ ($q = u/d$) can be easily derived by replacing $m_s \to 0$, $\langle\bar{s}s\rangle \to \langle\bar{q}q\rangle$, and $\langle g_s\bar{s}\sigma Gs\rangle \to \langle g_s\bar{q}\sigma Gq\rangle$. Note that we do not differentiate the up and down quarks in the calculations, so the states in the same isospin multiplet have the same extracted hadron mass; e.g., the two $\bar{q}qg$ states ($q = u/d$) with the quantum numbers $I^G J^{PC} = 0^+1^{-+}$ and 1^-1^{-+}, coupled by the same current $J^\mu_{1^{-+}}$, have the same extracted hadron mass.

We use the spectral density $\rho^{\bar{s}sg}_{1^{-+}}(s)$ given in Eq. (47) to perform numerical analyses. It is extracted from the current $J^\mu_{1^{-+}}$ with the quark-gluon content $\bar{s}sg$, which couples to the state

$$X_{1^{-+}} \equiv |\bar{s}sg; 1^{-+}\rangle. \tag{48}$$

We shall use the following values for various QCD parameters at the renormalization scale 2 GeV and the QCD scale $\Lambda_{\rm QCD} = 300$ MeV [1,112–119]:

$$\begin{aligned}
\alpha_s(Q^2) &= \frac{4\pi}{11\ln(Q^2/\Lambda^2_{\rm QCD})},\\
\langle\bar{q}q\rangle &= -(0.240 \pm 0.010)^3\ \mathrm{GeV}^3,\\
\langle\bar{s}s\rangle &= (0.8 \pm 0.1) \times \langle\bar{q}q\rangle,\\
\langle g_s\bar{q}\sigma Gq\rangle &= (0.8 \pm 0.2) \times \langle\bar{q}q\rangle\ \mathrm{GeV}^2,\\
\langle g_s\bar{s}\sigma Gs\rangle &= (0.8 \pm 0.2) \times \langle\bar{s}s\rangle,\\
\langle\alpha_s GG\rangle &= (6.35 \pm 0.35) \times 10^{-2}\ \mathrm{GeV}^4,\\
\langle g_s^3 G^3\rangle &= (8.2 \pm 1.0) \times \langle\alpha_s GG\rangle\ \mathrm{GeV}^2,\\
m_s &= 93^{+11}_{-5}\ \mathrm{MeV}.
\end{aligned} \tag{49}$$

Note that the value of the gluon condensate $\langle\alpha_s GG\rangle$ is taken from Ref. [119], which was written in 2018.

The mass $M_{1^{-+}}$ calculated by Eq. (44) depends on two free parameters: the Borel mass M_B and the threshold value s_0. We shall determine their proper working regions through three criteria: (a) the sufficiently good convergence of OPE, (b) the sufficiently large pole contribution, and (c) the sufficiently weak dependence of the mass $M_{1^{-+}}$ on these two parameters.

In order to have the sufficiently good convergence of OPE, we require the $\alpha_s \times g_s^2$ terms to be less than 5% and the $D = 6 + 8$ terms to be less than 10%:

$$\mathrm{CVG}_A \equiv \left|\frac{\Pi^{g_s^{n=4}}(\infty, M_B^2)}{\Pi(\infty, M_B^2)}\right| \le 5\%, \tag{50}$$

$$\mathrm{CVG}_B \equiv \left|\frac{\Pi^{\mathrm{D}=6+8}(\infty, M_B^2)}{\Pi(\infty, M_B^2)}\right| \le 10\%. \tag{51}$$

As depicted in Fig. 3, we determine the minimum Borel mass to be $M_B^2 \ge 2.26$ GeV^2, when setting $s_0 = 6.2$ GeV^2.

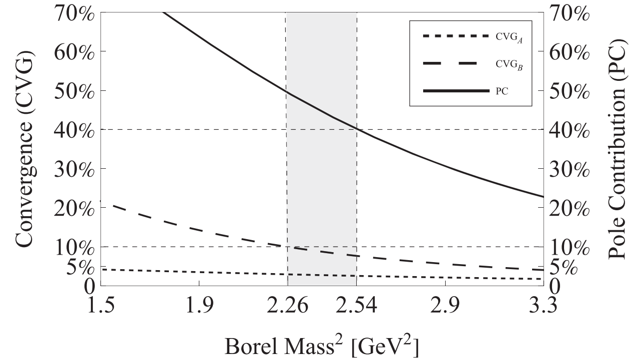

FIG. 3. CVG$_{A/B}$ and PC with respect to the Borel mass M_B, when setting $s_0 = 6.2$ GeV^2. These curves are obtained using the spectral density $\rho^{\bar{s}sg}_{1^{-+}}(s)$ extracted from the current $J^\mu_{1^{-+}}$ with the quark-gluon content $\bar{s}sg$.

In order to have the sufficiently large pole contribution, we require

$$\mathrm{PC} \equiv \left|\frac{\Pi(s_0, M_B^2)}{\Pi(\infty, M_B^2)}\right| \ge 40\%. \tag{52}$$

As depicted in Fig. 3, we determine the maximum Borel mass to be $M_B^2 \le 2.54$ GeV^2, when setting $s_0 = 6.2$ GeV^2.

Altogether the Borel window is determined to be $2.26\,\mathrm{GeV}^2 \le M_B^2 \le 2.54\,\mathrm{GeV}^2$, when setting $s_0 = 6.2\,\mathrm{GeV}^2$. Note that this Borel window is not so wide, and it was pointed in Ref. [120] that the narrow Borel window may indicate that the understanding of this state as a particle has limitations, so further studies on the hybrid states and particles are crucially demanded. We further change s_0 and find that there are nonvanishing Borel windows for $s_0 \ge s_0^{\min} = 5.1$ GeV^2. We choose s_0 to be about 10% larger and determine its working region to be 5.2 GeV$^2 \le s_0 \le 7.2$ GeV^2, where we calculate the mass and decay constant of the single-gluon hybrid state $X_{1^{-+}} \equiv |\bar{s}sg; 1^{-+}\rangle$ to be

$$M_{|\bar{s}sg;1^{-+}\rangle} = 1.84^{+0.14}_{-0.15}\ \mathrm{GeV}, \tag{53}$$

$$f_{|\bar{s}sg;1^{-+}\rangle} = 0.300^{+0.063}_{-0.058}\ \mathrm{GeV}^4. \tag{54}$$

Their uncertainties come from M_B and s_0 as well as various QCD parameters listed in Eq. (49). We show the mass $M_{|\bar{s}sg;1^{-+}\rangle}$ in Fig. 4 with respect to the threshold value s_0 and the Borel mass M_B. In the left panel, the mass dependence on s_0 is moderate inside the working region 5.2 GeV$^2 \le s_0 \le 7.2$ GeV^2. In the right panel, the mass curves are sufficiently stable inside the Borel window 2.26 GeV$^2 \le M_B^2 \le 2.54$ GeV^2.

Similarly, we perform numerical analyses using the other single-gluon hybrid currents with the quark-gluon contents $\bar{q}qg$ ($q = u/d$) and $\bar{s}sg$. The obtained results are

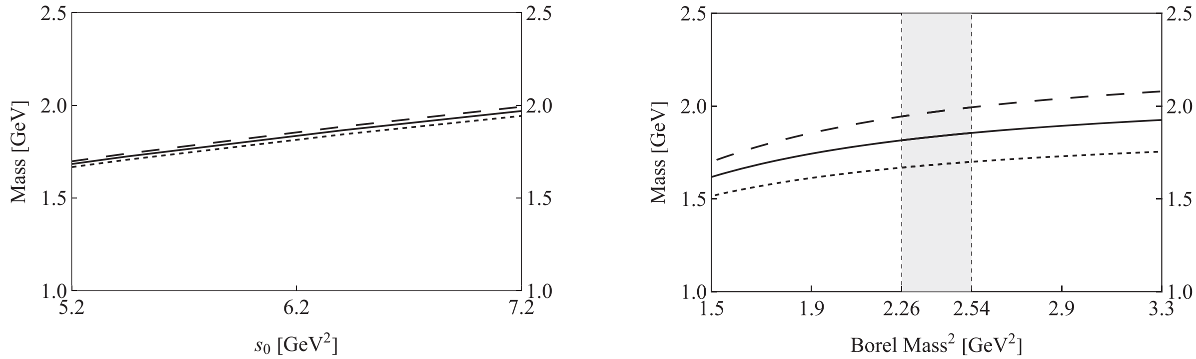

FIG. 4. Mass of the single-gluon hybrid state $|\bar{s}sg;1^{-+}\rangle$ with respect to the threshold value s_0 (left) and the Borel mass M_B (right). In the left panel, the dotted, solid, and dashed curves are obtained by setting $M_B^2 = 2.26$, 2.40, and 2.54 GeV^2, respectively. In the right panel, the dotted, solid, and dashed curves are obtained by setting $s_0 = 5.2$, 6.2, and 7.2 GeV^2, respectively. These curves are obtained using the spectral density $\rho^{\bar{s}sg}_{1^{-+}}(s)$ extracted from the current $J^\mu_{1^{-+}}$ with the quark-gluon content $\bar{s}sg$.

summarized in Tables I and II. Especially, we use the current $J^\mu_{1^{-+}}$ with the quark-gluon content $\bar{q}qg$ $(q = u/d)$ to calculate the mass and decay constant of the single-gluon hybrid state $|\bar{q}qg;1^{-+}\rangle$ to be

$$M_{|\bar{q}qg;1^{-+}\rangle} = 1.67^{+0.15}_{-0.17}\ \text{GeV}, \tag{55}$$

$$f_{|\bar{q}qg;1^{-+}\rangle} = 0.243^{+0.057}_{-0.052}\ \text{GeV}^4. \tag{56}$$

TABLE I. QCD sum rule results for the single-gluon hybrid states $|\bar{q}qg;J^{PC}\rangle$, extracted from the single-gluon hybrid currents given in Eqs. (7)–(14) and (19)–(30) with the quark-gluon contents $\bar{q}qg$ $(q = u/d)$. The results for the isoscalar state $|\bar{q}qg;0^G J^{PC}\rangle$ and the isovector state $|\bar{q}qg;1^G J^{PC}\rangle$ within the same isospin multiplet are the same as each other.

			Working regions				
State $[J^{PC}]$	Current	$s_0^{\min}$ [GeV^2]	M_B^2 [GeV^2]	s_0 [GeV^2]	Pole [%]	Mass [GeV]	Decay constant
$\vert\bar{q}qg;1^{--}\rangle$	$J^{\alpha\beta}_{1^{--}}$	4.2	2.03–2.48	5.5	40–54	$1.80^{+0.13}_{-0.16}$	$0.051^{+0.004}_{-0.004}$ GeV^3
$\vert\bar{q}qg;1^{+-}\rangle$	$\tilde{J}^{\alpha\beta}_{1^{+-}}$	16.2	3.61–4.58	18.0	40–53	$4.05^{+0.24}_{-0.12}$	$0.063^{+0.020}_{-0.020}$ GeV^3
$\vert\bar{q}qg;1^{+-}\rangle$	$J^{\alpha\beta}_{1^{+-}}$	5.0	2.29–2.45	5.5	40–45	$1.84^{+0.12}_{-0.14}$	$0.049^{+0.004}_{-0.004}$ GeV^3
$\vert\bar{q}qg;1^{--}\rangle$	$\tilde{J}^{\alpha\beta}_{1^{--}}$	16.3	3.52–4.56	18.0	40–53	$4.09^{+0.29}_{-0.14}$	$0.064^{+0.021}_{-0.020}$ GeV^3
$\vert\bar{q}qg;0^{++}\rangle$	$J^{\mu\to 0}_{1^{-+}}$	20.6	5.11–6.59	24.0	40–56	$4.45^{+0.22}_{-0.17}$	$0.124^{+0.032}_{-0.036}$ GeV^3
$\vert\bar{q}qg;0^{-+}\rangle$	$\tilde{J}^{\mu\to 0}_{1^{++}}$	7.7	3.58–3.81	8.5	40–45	$2.14^{+0.17}_{-0.19}$	$0.105^{+0.005}_{-0.004}$ GeV^3
$\vert\bar{q}qg;0^{--}\rangle$	$J^{\mu\to 0}_{1^{+-}}$	21.6	5.48–6.52	24.0	40–50	$4.49^{+0.21}_{-0.14}$	$0.123^{+0.032}_{-0.037}$ GeV^3
$\vert\bar{q}qg;0^{+-}\rangle$	$\tilde{J}^{\mu\to 0}_{1^{--}}$	7.1	3.32–3.73	8.5	40–49	$2.16^{+0.16}_{-0.19}$	$0.100^{+0.005}_{-0.005}$ GeV^3
$\vert\bar{q}qg;1^{-+}\rangle$	$J^{\mu}_{1^{-+}}$	4.8	2.19–2.28	5.2	40–43	$1.67^{+0.15}_{-0.17}$	$0.243^{+0.057}_{-0.052}$ GeV^4
$\vert\bar{q}qg;1^{++}\rangle$	$\tilde{J}^{\mu}_{1^{++}}$	13.8	3.59–4.10	15.0	40–48	$3.54^{+0.16}_{-0.12}$	$1.370^{+0.494}_{-0.450}$ GeV^4
$\vert\bar{q}qg;1^{+-}\rangle$	$J^{\mu}_{1^{+-}}$	4.6	2.10–2.27	5.2	40–46	$1.68^{+0.14}_{-0.16}$	$0.242^{+0.055}_{-0.051}$ GeV^4
$\vert\bar{q}qg;1^{--}\rangle$	$\tilde{J}^{\mu}_{1^{--}}$	13.7	3.57–4.10	15.0	40–49	$3.53^{+0.16}_{-0.12}$	$1.366^{+0.493}_{-0.450}$ GeV^4
$\vert\bar{q}qg;0^{++}\rangle$	$J_{0^{++}}$	11.1	3.48–3.91	12.5	40–49	$2.94^{+0.20}_{-0.25}$	$2.893^{+1.029}_{-0.948}$ GeV^4
$\vert\bar{q}qg;0^{-+}\rangle$	$J_{0^{-+}}$	11.1	3.47–3.92	12.5	40–49	$2.93^{+0.20}_{-0.25}$	$2.882^{+1.026}_{-0.945}$ GeV^4
$\vert\bar{q}qg;1^{++}\rangle$	$J^{\alpha\beta}_{1^{++}}$	5.8	1.84–2.06	6.5	40–48	$2.11^{+0.17}_{-0.21}$	$0.056^{+0.012}_{-0.013}$ GeV^3
$\vert\bar{q}qg;1^{-+}\rangle$	$\tilde{J}^{\alpha\beta}_{1^{-+}}$	5.5	1.81–2.00	6.2	40–48	$2.00^{+0.13}_{-0.16}$	$0.055^{+0.007}_{-0.008}$ GeV^3
$\vert\bar{q}qg;1^{-+}\rangle$	$J^{\alpha\beta}_{1^{-+}}$	5.5	1.81–2.00	6.2	40–48	$2.00^{+0.13}_{-0.16}$	$0.055^{+0.007}_{-0.008}$ GeV^3
$\vert\bar{q}qg;1^{++}\rangle$	$\tilde{J}^{\alpha\beta}_{1^{++}}$	5.8	1.84–2.06	6.5	40–48	$2.11^{+0.17}_{-0.21}$	$0.056^{+0.012}_{-0.013}$ GeV^3
$\vert\bar{q}qg;2^{++}\rangle$	$J^{\alpha_1\beta_1,\alpha_2\beta_2}_{2^{++}}$	8.6	3.11–3.37	9.5	40–46	$2.44^{+0.20}_{-0.24}$	…
$\vert\bar{q}qg;2^{-+}\rangle$	$\tilde{J}^{\alpha_1\beta_1,\alpha_2\beta_2}_{2^{-+}}$	12.7	2.54–3.60	14.0	40–54	$3.68^{+0.62}_{-0.18}$	…
$\vert\bar{q}qg;2^{-+}\rangle$	$J^{\alpha_1\beta_1,\alpha_2\beta_2}_{2^{-+}}$	8.3	3.07–3.41	9.5	40–48	$2.40^{+0.21}_{-0.25}$	…
$\vert\bar{q}qg;2^{++}\rangle$	$\tilde{J}^{\alpha_1\beta_1,\alpha_2\beta_2}_{2^{++}}$	11.7	2.47–3.70	14.0	40–63	$3.46^{+0.27}_{-0.11}$	…

TABLE II. QCD sum rule results for the single-gluon hybrid states $|\bar{s}sg; J^{PC}\rangle$, extracted from the single-gluon hybrid currents given in Eqs. (7)–(14) and (19)–(30) with the quark-gluon contents $\bar{s}sg$.

			Working regions				
State $[J^{PC}]$	Current	$s_0^{\min}$ [GeV^2]	M_B^2 [GeV^2]	s_0 [GeV^2]	Pole [%]	Mass [GeV]	Decay constant
$\|\bar{s}sg; 1^{--}\rangle$	$J^{\alpha\beta}_{1^{--}}$	4.3	2.07–2.80	6.5	40–63	$1.94^{+0.20}_{-0.21}$	$0.054^{+0.013}_{-0.016}$ GeV^3
$\|\bar{s}sg; 1^{+-}\rangle$	$\tilde{J}^{\alpha\beta}_{1^{+-}}$	16.2	3.60–5.40	20.0	40–65	$4.06^{+0.26}_{-0.16}$	$0.071^{+0.019}_{-0.020}$ GeV^3
$\|\bar{s}sg; 1^{+-}\rangle$	$J^{\alpha\beta}_{1^{+-}}$	5.9	2.54–2.72	6.5	40–45	$2.01^{+0.17}_{-0.20}$	$0.050^{+0.005}_{-0.006}$ GeV^3
$\|\bar{s}sg; 1^{--}\rangle$	$\tilde{J}^{\alpha\beta}_{1^{--}}$	16.9	3.73–5.30	20.0	40–61	$4.12^{+0.26}_{-0.13}$	$0.070^{+0.019}_{-0.020}$ GeV^3
$\|\bar{s}sg; 0^{++}\rangle$	$J^{\mu\to 0}_{1^{-+}}$	20.7	5.18–7.35	26.0	40–63	$4.50^{+0.23}_{-0.22}$	$0.136^{+0.030}_{-0.034}$ GeV^3
$\|\bar{s}sg; 0^{-+}\rangle$	$\tilde{J}^{\mu\to 0}_{1^{++}}$	7.2	3.45–4.08	9.5	40–53	$2.26^{+0.21}_{-0.24}$	$0.107^{+0.007}_{-0.005}$ GeV^3
$\|\bar{s}sg; 0^{--}\rangle$	$J^{\mu\to 0}_{1^{+-}}$	21.6	5.36–7.23	26.0	40–59	$4.57^{+0.22}_{-0.19}$	$0.134^{+0.031}_{-0.035}$ GeV^3
$\|\bar{s}sg; 0^{+-}\rangle$	$\tilde{J}^{\mu\to 0}_{1^{--}}$	7.5	3.41–3.98	9.5	40–52	$2.30^{+0.20}_{-0.24}$	$0.101^{+0.007}_{-0.006}$ GeV^3
$\|\bar{s}sg; 1^{-+}\rangle$	$J^{\mu}_{1^{-+}}$	5.1	2.26–2.54	6.2	40–49	$1.84^{+0.14}_{-0.15}$	$0.300^{+0.063}_{-0.058}$ GeV^4
$\|\bar{s}sg; 1^{++}\rangle$	$\tilde{J}^{\mu}_{1^{++}}$	14.1	3.64–4.80	17.0	40–58	$3.65^{+0.17}_{-0.17}$	$1.678^{+0.530}_{-0.502}$ GeV^4
$\|\bar{s}sg; 1^{+-}\rangle$	$J^{\mu}_{1^{+-}}$	3.9	1.85–2.43	6.0	40–62	$1.82^{+0.13}_{-0.15}$	$0.278^{+0.059}_{-0.056}$ GeV^4
$\|\bar{s}sg; 1^{--}\rangle$	$\tilde{J}^{\mu}_{1^{--}}$	13.8	3.50–4.80	17.0	40–61	$3.64^{+0.17}_{-0.17}$	$1.662^{+0.526}_{-0.498}$ GeV^4
$\|\bar{s}sg; 0^{++}\rangle$	$J_{0^{++}}$	11.5	3.53–4.33	14.0	40–55	$3.11^{+0.22}_{-0.27}$	$3.535^{+1.338}_{-1.242}$ GeV^4
$\|\bar{s}sg; 0^{-+}\rangle$	$J_{0^{-+}}$	11.3	3.51–4.36	14.0	40–56	$3.08^{+0.23}_{-0.28}$	$3.509^{+1.328}_{-1.233}$ GeV^4
$\|\bar{s}sg; 1^{++}\rangle$	$J^{\alpha\beta}_{1^{++}}$	6.6	1.95–2.27	7.5	40–51	$2.34^{+0.14}_{-0.16}$	$0.061^{+0.012}_{-0.014}$ GeV^3
$\|\bar{s}sg; 1^{-+}\rangle$	$\tilde{J}^{\alpha\beta}_{1^{-+}}$	5.5	1.82–2.25	7.0	40–57	$2.08^{+0.18}_{-0.24}$	$0.061^{+0.010}_{-0.010}$ GeV^3
$\|\bar{s}sg; 1^{-+}\rangle$	$J^{\alpha\beta}_{1^{-+}}$	5.5	1.82–2.25	7.0	40–57	$2.08^{+0.18}_{-0.24}$	$0.061^{+0.010}_{-0.010}$ GeV^3
$\|\bar{s}sg; 1^{++}\rangle$	$\tilde{J}^{\alpha\beta}_{1^{++}}$	6.6	1.95–2.27	7.5	40–51	$2.34^{+0.14}_{-0.16}$	$0.061^{+0.012}_{-0.014}$ GeV^3
$\|\bar{s}sg; 2^{++}\rangle$	$J^{\alpha_1\beta_1,\alpha_2\beta_2}_{2^{++}}$	9.2	3.22–3.60	10.5	40–49	$2.59^{+0.19}_{-0.23}$	...
$\|\bar{s}sg; 2^{-+}\rangle$	$\tilde{J}^{\alpha_1\beta_1,\alpha_2\beta_2}_{2^{-+}}$	13.4	2.55–4.29	16.0	40–66	$3.72^{+0.72}_{-0.13}$	...
$\|\bar{s}sg; 2^{-+}\rangle$	$J^{\alpha_1\beta_1,\alpha_2\beta_2}_{2^{-+}}$	8.1	3.04–3.72	10.5	40–56	$2.51^{+0.20}_{-0.24}$	...
$\|\bar{s}sg; 2^{++}\rangle$	$\tilde{J}^{\alpha_1\beta_1,\alpha_2\beta_2}_{2^{++}}$	11.8	2.36–4.47	16.0	40–78	$3.54^{+0.42}_{-0.16}$	...

IV. DECAY PROPERTIES OF THE $J^{PC} = 1^{-+}$ HYBRID STATES

In this section, we systematically study the decay properties of the $J^{PC} = 1^{-+}$ hybrid states, whose masses and decay constants have been calculated in the previous section. Since we do not differentiate the up and down quarks within the QCD sum rule method, the masses and decay constants of the states in the same isospin multiplet are calculated to be the same:

$$
\begin{aligned}
M_{|\bar{q}qg;1^-1^{-+}\rangle} = M_{|\bar{q}qg;0^+1^{-+}\rangle} &= 1.67^{+0.15}_{-0.17}\ \text{GeV},\\
f_{|\bar{q}qg;1^-1^{-+}\rangle} = f_{|\bar{q}qg;0^+1^{-+}\rangle} &= 0.243^{+0.057}_{-0.052}\ \text{GeV}^4,\\
M_{|\bar{s}sg;0^+1^{-+}\rangle} &= 1.84^{+0.14}_{-0.15}\ \text{GeV},\\
f_{|\bar{s}sg;0^+1^{-+}\rangle} &= 0.300^{+0.063}_{-0.058}\ \text{GeV}^4.
\end{aligned}
$$

As shown in Fig. 5(a), a single-gluon hybrid state can decay after exciting one $\bar{q}q/\bar{s}s$ pair from the valence gluon, followed by reorganizing two color-octet $\bar{q}q/\bar{s}s$ pairs into two color-singlet mesons. This decay process has been systematically studied in Refs. [109,110] for the $J^{PC} = 1^{-+}$ hybrid states through the QCD sum rule method, and in the present study we update these calculations. Besides the "normal" decay process depicted in Fig. 5(a), there also exist the "abnormal" decay processes depicted in Figs. 5(b) and 5(c), where the $\eta^{(\prime)}$ mesons are produced by the QCD axial anomaly. These abnormal decay processes have been systematically studied in Ref. [111], and in the present study we also update these calculations.

We shall use the decay modes $\pi_1 \equiv |\bar{q}qg; 1^-1^{-+}\rangle \to \rho\pi$ and $\eta_1 \equiv |\bar{s}sg; 0^+1^{-+}\rangle \xrightarrow{c} \eta\eta'$ as two examples to separately study the normal and abnormal decay processes in the following subsections.

A. Normal decay process

In this subsection, we use the decay mode

$$
\pi_1 \equiv |\bar{q}qg; 1^-1^{-+}\rangle \to \rho\pi \tag{57}
$$

as an example to study the normal decay process depicted in Fig. 5(a) through the three-point correlation function

$$
T_{\mu\nu}(p,k,q) = \int d^4x d^4y e^{ikx} e^{iqy} \times \langle 0|\mathbb{T}[J^{\rho^-}_{\nu}(x) J^{\pi^+}_{5}(y) J^{\mu\dagger}_{1^{-+}}(0)]|0\rangle, \tag{58}
$$

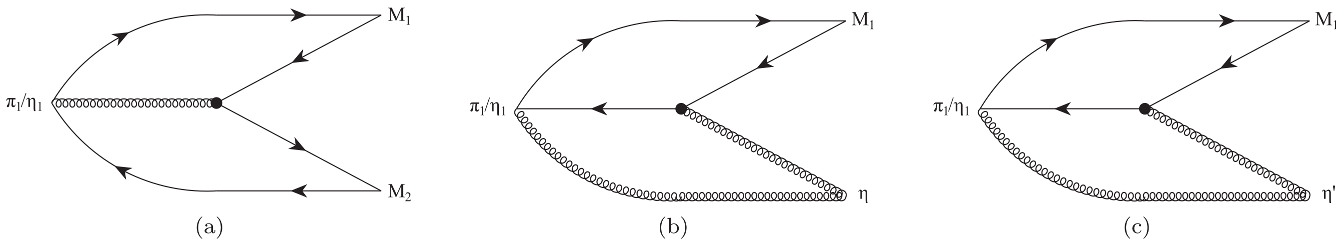

FIG. 5. Decay mechanisms of the single-gluon hybrid states through (a) the normal process with one quark-antiquark pair excited from the valence gluon and (b),(c) the abnormal processes with the η/η' produced by the QCD axial anomaly.

where p, k, and q are the momenta of $\pi_1 \equiv |\bar{q}qg; 1^-1^{-+}\rangle$, ρ^-, and π^+, respectively. The current $J^\mu_{1^{-+}}$ has been defined in Eq. (11), and we select the isovector neutral-charged one

$$J^\mu_{1^{-+}} \to \frac{1}{\sqrt{2}}(\bar{u}_a \lambda_n^{ab} \gamma_\beta u_b - \bar{d}_a \lambda_n^{ab} \gamma_\beta d_b) g_s G_n^{\mu\beta}. \quad (59)$$

The negative-charged vector current $J^{\rho^-}_\mu = \bar{u}\gamma_\mu d$ and the positive-charged pseudoscalar current $J^{\pi^+}_5 = \bar{d}\gamma_5 u$, respectively, couple to the vector meson ρ^- and the pseudoscalar meson π^+ through

$$\langle 0|J^{\rho^-}_\mu|\rho^-(k,\epsilon)\rangle = m_\rho f_\rho \epsilon_\mu, \quad (60)$$

$$\langle 0|J^{\pi^+}_5|\pi(q)\rangle = f'_\pi = \frac{2i\langle\bar{q}q\rangle}{f_\pi}, \quad (61)$$

with [87,121,122]

$$\begin{aligned} m_\pi &= 140\ \text{MeV}, & f_\pi &= 131\ \text{MeV}, \\ m_\rho &= 770\ \text{MeV}, & f_\rho &= 220\ \text{MeV}. \end{aligned} \quad (62)$$

At the phenomenological side, we write $T_{\mu\nu}(p,k,q)$ as

$$T_{\mu\nu}(p,k,q) = g_{\rho\pi} \epsilon_{\mu\nu\alpha\beta} q^\alpha k^\beta \frac{f_{\pi_1} f_\rho m_\rho f'_\pi}{(m^2_{\pi_1} - p^2)(m^2_\rho - k^2)(m^2_\pi - q^2)}, \quad (63)$$

where the coupling constant $g_{\rho\pi}$ is defined through the Lagrangian

$$\mathcal{L} = g_{\rho\pi} \epsilon_{\mu\nu\alpha\beta} \pi_1^{0\mu} \partial^\alpha \pi^+ \partial^\beta \rho^{-\nu} + \cdots. \quad (64)$$

At the QCD side, we calculate $T_{\mu\nu}(p,k,q)$ using the method of operator product expansion. We work at the pion pole and choose the terms divergent at the $q^2 \to 0$ limit to derive

$$T_{\mu\nu}(p,k,q) = \frac{\epsilon_{\mu\nu\alpha\beta} q^\alpha k^\beta}{q^2} \left(\frac{\langle g_s \bar{q}\sigma G q\rangle}{6\sqrt{2}} \left(\frac{3}{p^2} + \frac{1}{k^2} \right) - \frac{\langle\bar{q}q\rangle\langle g_s^2 GG\rangle}{18\sqrt{2}} \left(\frac{1}{p^4} + \frac{1}{k^4} \right) \right). \quad (65)$$

We compare Eqs. (63) and (65) to calculate the coupling constant $g_{\rho\pi}$. After setting $p^2 = k^2$ and performing the Borel transformation once $\mathcal{B}(p^2 = k^2 \to T^2)$, we arrive at

$$\begin{aligned} &- g_{\rho\pi} \frac{f_{\pi_1} f_\rho m_\rho f'_\pi}{m^2_\rho - m^2_{\pi_1}} (e^{-m^2_{\pi_1}/T^2} - e^{-m^2_\rho/T^2}) \\ &= - \frac{2\langle g\bar{q}\sigma G q\rangle}{3\sqrt{2}} - \frac{\langle\bar{q}q\rangle\langle g_s^2 GG\rangle}{9\sqrt{2}} \frac{1}{T^2}. \end{aligned} \quad (66)$$

The formula of the decay width reads

$$\Gamma(\pi_1^0 \to \rho^+\pi^- + \rho^-\pi^+) = 2 \times \frac{g^2_{\rho\pi}}{12\pi} |\vec{q}_\pi|^3, \quad (67)$$

where $\vec{q}_\pi$ is the three-momentum of the final state π. Numerically, we obtain

$$g_{\rho\pi} = 4.08^{+2.40}_{-1.83}\ \text{GeV}^{-1}, \quad (68)$$

$$\Gamma(\pi_1 \to \rho\pi) = 242^{+310}_{-179}\ \text{MeV}. \quad (69)$$

B. Abnormal decay process

In this subsection, we use the decay mode

$$\eta_1 \equiv |\bar{s}sg; 0^+1^{-+}\rangle \xrightarrow{c} \eta\eta' \quad (70)$$

as an example to study the abnormal decay process depicted in Fig. 5(c), with η' produced by the QCD $U(1)_A$ anomaly. Before doing this, let us shortly introduce the two-angle mixing formalism to describe the η and η' mesons [123–132]:

$$\begin{aligned} |\eta\rangle &= \cos\theta_8|\eta_8\rangle - \sin\theta_0|\eta_0\rangle + \cdots, \\ |\eta'\rangle &= \sin\theta_8|\eta_8\rangle + \cos\theta_0|\eta_0\rangle + \cdots, \end{aligned} \quad (71)$$

with

$$\begin{aligned} |\eta_8\rangle &= |u\bar{u} + d\bar{d} - 2s\bar{s}\rangle/\sqrt{6}, \\ |\eta_0\rangle &= |u\bar{u} + d\bar{d} + s\bar{s}\rangle/\sqrt{3}, \end{aligned} \quad (72)$$

and $\cdots$ are contributions from the pseudoscalar glueballs and charmonium, etc.

The octet and singlet axial-vector currents are defined as

$$A_\mu^8 = (\bar{u}\gamma_\mu\gamma_5 u + \bar{d}\gamma_\mu\gamma_5 d - 2\bar{s}\gamma_\mu\gamma_5 s)/\sqrt{12},$$
$$A_\mu^0 = (\bar{u}\gamma_\mu\gamma_5 u + \bar{d}\gamma_\mu\gamma_5 d + \bar{s}\gamma_\mu\gamma_5 s)/\sqrt{6}. \quad (73)$$

These two currents couple to the η and η' mesons through

$$\langle 0|A_\mu^a|P(k)\rangle = ik_\mu f_P^a, \quad (74)$$

where f_P^a $(a = 8, 0; P = \eta, \eta')$ is the matrix for the decay constants, defined as

$$\begin{pmatrix} f_\eta^8 & f_\eta^0 \\ f_{\eta'}^8 & f_{\eta'}^0 \end{pmatrix} = \begin{pmatrix} f_8 \cos\theta_8 & -f_0 \sin\theta_0 \\ f_8 \sin\theta_8 & f_0 \cos\theta_0 \end{pmatrix}. \quad (75)$$

To simply our notations, we further construct the axial-vector currents

$$J_\mu^\eta = A_\mu^8 + t_\eta A_\mu^0, \quad (76)$$

$$J_\mu^{\eta'} = A_\mu^8 + t_{\eta'} A_\mu^0, \quad (77)$$

which couple to the η and η' mesons through

$$\langle 0|J_\mu^\eta|\eta(k)\rangle = ik_\mu g_\eta,$$
$$\langle 0|J_\mu^{\eta'}|\eta'(k)\rangle = ik_\mu g_{\eta'},$$
$$\langle 0|J_\mu^\eta|\eta'(k)\rangle = \langle 0|J_\mu^{\eta'}|\eta(k)\rangle = 0, \quad (78)$$

with

$$g_\eta = f_\eta^8 - f_\eta^0 f_{\eta'}^8/f_{\eta'}^0,$$
$$g_{\eta'} = f_{\eta'}^8 - f_{\eta'}^0 f_\eta^8/f_\eta^0,$$
$$t_\eta = -f_{\eta'}^8/f_{\eta'}^0,$$
$$t_{\eta'} = -f_\eta^8/f_\eta^0. \quad (79)$$

We shall use the following values in the calculations [133,134]:

$$\theta_8 = -22.2°,$$
$$\theta_0 = -9.1°,$$
$$f_8 = 168 \text{ MeV},$$
$$f_0 = 157 \text{ MeV}. \quad (80)$$

The conversion of the gluons into the η and η' mesons can be described through the QCD $U(1)_A$ anomaly as [133,135–139]

$$\langle 0|\frac{\alpha_s}{4\pi} G_n^{\alpha\beta} \tilde{G}_{n,\alpha\beta}|\eta\rangle = m_\eta^2 f_\eta, \quad (81)$$

$$\langle 0|\frac{\alpha_s}{4\pi} G_n^{\alpha\beta} \tilde{G}_{n,\alpha\beta}|\eta'\rangle = m_{\eta'}^2 f_{\eta'}, \quad (82)$$

with

$$f_\eta = \frac{f_8}{\sqrt{6}}\cos\theta_8 - \frac{f_0}{\sqrt{3}}\sin\theta_0, \quad (83)$$

$$f_{\eta'} = \frac{f_8}{\sqrt{6}}\sin\theta_8 + \frac{f_0}{\sqrt{3}}\cos\theta_0. \quad (84)$$

To study the abnormal decay process $\eta_1 \equiv |\bar{s}sg; 0^+1^{-+}\rangle \xrightarrow{c} \eta\eta'$ depicted in Fig. 5(c), with η' produced by the QCD $U(1)_A$ anomaly, we consider the three-point correlation function:

$$T'_{\mu\nu}(p,k,q) = \int d^4x e^{-ikx}\langle 0|\mathbb{T}[J^\mu_{1^{-+}}(0) J_\nu^{\eta\dagger}(x)]|\eta'\rangle, \quad (85)$$

where p, k, and q are the momenta of $\eta_1 \equiv |\bar{s}sg; 0^+1^{-+}\rangle$, η, and η', respectively. The current J_ν^η has been defined in Eq. (76). The current $J^\mu_{1^{-+}}$ has been defined in Eq. (11), and we set its quark content to be

$$J^\mu_{1^{-+}} \to \bar{s}_a \lambda_n^{ab} \gamma_\beta s_b g_s G_n^{\mu\beta}. \quad (86)$$

At the phenomenological side, we write $T'_{\mu\nu}(p,k,q)$ as

$$T'_{\mu\nu}(p,k,q) = g_{\eta\eta'} k_\mu k_\nu \frac{f_{\eta_1} g_\eta}{(m_{\eta_1}^2 - p^2)(m_\eta^2 - k^2)}, \quad (87)$$

where the coupling constant $g_{\eta\pi}$ is defined through the Lagrangian

$$\mathcal{L}' = g_{\eta\eta'} \eta_1^\mu (\partial_\mu \eta)\eta'. \quad (88)$$

At the QCD side, we calculate $T'_{\mu\nu}(p,k,q)$ using the method of operator product expansion to be

$$T'_{\mu\nu}(p,k,q) = \theta_s k_\mu k_\nu \left(-\frac{2m_{\eta'}^2 f_{\eta'}}{3k^2} - \frac{4\pi^2 m_{\eta'}^2 f_{\eta'} m_s \langle\bar{s}s\rangle}{3k^6}\right), \quad (89)$$

where $\theta_s = -1/\sqrt{3} + t_\eta/\sqrt{6}$ describes the $s\bar{s}$ component contained in the current J_ν^η.

After setting $p^2 = k^2$ and performing the Borel transformation once $\mathcal{B}(p^2 = k^2 \to T^2)$, we arrive at

$$g_{\eta\eta'} \frac{f_{\eta_1} g_\eta}{m_{\eta_1}^2 - m_\eta^2} \left(e^{-m_\eta^2/M_B^2} - e^{-m_{\eta_1}^2/M_B^2}\right) = \frac{2\theta_s m_{\eta'}^2 f_{\eta'}}{3} + \frac{2\pi^2 \theta_s m_{\eta'}^2 f_{\eta'} m_s \langle\bar{s}s\rangle}{3} \frac{1}{M_B^4}. \quad (90)$$

The formula of the decay width reads

$$\Gamma(\eta_1 \to \eta\eta') = \frac{g_{\eta\eta'}^2}{24\pi m_{\eta_1}^2} |\vec{q}_\eta|^3, \quad (91)$$

TABLE III. Partial decay widths of the hybrid states $|\bar{q}qg;1^-1^{-+}\rangle$, $|\bar{q}qg;0^+1^{-+}\rangle$, and $|\bar{s}sg;0^+1^{-+}\rangle$, in units of MeV. $\Gamma(\pi_1/\eta_1 \xrightarrow{a,b,c} M_1M_2)$ are related to the processes depicted in Figs. 5(a)–5(c), respectively. We simply sum over the partial decay widths to obtain the total decay widths, as listed in the last row. Note that the decay channels $\pi_1 \xrightarrow{b,c} \eta\pi/\eta'\pi$ and $\pi_1/\eta_1 \to K^*(892)\bar{K}/K_1(1270)\bar{K}/K^*(892)\bar{K}^*(892)$ have not been investigated in our previous QCD sum rule studies [109–111].

Channel	$\vert\bar{q}qg;1^-1^{-+}\rangle$ $M = 1.67^{+0.15}_{-0.17}$ GeV	$\vert\bar{q}qg;0^+1^{-+}\rangle$ $M = 1.67^{+0.15}_{-0.17}$ GeV	$\vert\bar{s}sg;0^+1^{-+}\rangle$ $M = 1.84^{+0.14}_{-0.15}$ GeV
$\pi_1/\eta_1 \to \rho\pi$	242^{+310}_{-179}	...	...
$\pi_1/\eta_1 \to b_1(1235)\pi$	$14.5^{+25.9}_{-13.9}$	...	...
$\pi_1/\eta_1 \to f_1(1285)\pi$	$35.9^{+53.9}_{-36.4}$	...	...
$\pi_1/\eta_1 \to \eta\pi$	$2.3^{+2.5}_{-1.2}$	...	...
$\pi_1/\eta_1 \xrightarrow{b} \eta\pi$	$57.8^{+65.0}_{-31.4}$	...	...
$\pi_1/\eta_1 \to \eta'\pi$	$0.43^{+0.50}_{-0.28}$	...	...
$\pi_1/\eta_1 \xrightarrow{c} \eta'\pi$	149^{+162}_{-78}	...	...
$\pi_1/\eta_1 \to a_1(1260)\pi$	...	$79.5^{+112.4}_{-74.9}$	...
$\pi_1/\eta_1 \xrightarrow{a} \eta\eta'$	...	$0.07^{+0.12}_{-0.07}$	$0.93^{+1.04}_{-0.69}$
$\pi_1/\eta_1 \xrightarrow{b} \eta\eta'$	...	$1.62^{+2.13}_{-1.61}$	$1.64^{+1.51}_{-1.01}$
$\pi_1/\eta_1 \xrightarrow{c} \eta\eta'$	...	$11.5^{+11.7}_{-11.5}$	$5.0^{+4.6}_{-3.1}$
$\pi_1/\eta_1 \to K^*(892)\bar{K} + \text{c.c.}$	$25.3^{+34.7}_{-24.7}$	$25.3^{+34.7}_{-24.7}$	$73.9^{+85.7}_{-58.0}$
$\pi_1/\eta_1 \to K_1(1270)\bar{K} + \text{c.c.}$	...	...	$14.6^{+19.8}_{-14.6}$
$\pi_1/\eta_1 \to K^*(892)\bar{K}^*(892)$	...	...	$0.08^{+0.39}_{-0.08}$
Sum	530^{+540}_{-330}	120^{+160}_{-110}	100^{+110}_{-80}

where $\vec{q}_\eta$ is the three-momentum of the final state η. Numerically, we obtain

$$g_{\eta\eta'} = 3.08^{+1.30}_{-0.91}, \tag{92}$$

$$\Gamma(\eta_1 \xrightarrow{c} \eta\eta') = 5.0^{+4.6}_{-3.1}\ \text{MeV}. \tag{93}$$

Similarly, we study the other normal and abnormal decay processes. The obtained results are summarized in Table III.

V. SUMMARY AND DISCUSSIONS

In this paper, we study the single-gluon hybrid states with various (exotic) quantum numbers. We systematically construct 24 single-gluon hybrid currents and use 18 of them to perform QCD sum rule analyses. We calculate the masses of 44 single-gluon hybrid states with the quark-gluon contents $\bar{q}qg$ ($q = u/d$) and $\bar{s}sg$. The obtained results are summarized in Tables I and II. Especially, the masses and decay constants of the $J^{PC} = 1^{-+}$ hybrid states are extracted from the current $J^\mu_{1^{-+}}$ given in Eq. (11) to be

$$\begin{aligned} M_{|\bar{q}qg;1^{-+}\rangle} &= 1.67^{+0.15}_{-0.17}\ \text{GeV}, \\ f_{|\bar{q}qg;1^{-+}\rangle} &= 0.243^{+0.057}_{-0.052}\ \text{GeV}^4, \\ M_{|\bar{s}sg;1^{-+}\rangle} &= 1.84^{+0.14}_{-0.15}\ \text{GeV}, \\ f_{|\bar{s}sg;1^{-+}\rangle} &= 0.300^{+0.063}_{-0.058}\ \text{GeV}^4. \end{aligned}$$

Since we do not differentiate the up and down quarks within the QCD sum rule method, the masses and decay constants of the states in the same isospin multiplet are calculated to be the same:

$$\begin{aligned} M_{|\bar{q}qg;1^-1^{-+}\rangle} = M_{|\bar{q}qg;0^+1^{-+}\rangle} &= 1.67^{+0.15}_{-0.17}\ \text{GeV}, \\ f_{|\bar{q}qg;1^-1^{-+}\rangle} = f_{|\bar{q}qg;0^+1^{-+}\rangle} &= 0.243^{+0.057}_{-0.052}\ \text{GeV}^4, \\ M_{|\bar{s}sg;0^+1^{-+}\rangle} &= 1.84^{+0.14}_{-0.15}\ \text{GeV}, \\ f_{|\bar{s}sg;0^+1^{-+}\rangle} &= 0.300^{+0.063}_{-0.058}\ \text{GeV}^4. \end{aligned}$$

There have been a lot of lattice QCD calculations on the $I^GJ^{PC} = 1^-1^{-+}$ hybrid state in the past 50 years [41,42,140–143], and, especially, the Hadron Spectrum Collaboration have performed exhaustive analyses [8,45,64,65,144–146]. Meyer and Swanson summarized these results, and the naive extrapolation of its mass, calculated by lattice QCD, to the physical pion mass turns out to be approximately 1.6 GeV [6]. Therefore, our QCD sum rule calculation is well consistent with the lattice QCD calculations.

Based on the mass calculations, we systematically study the decay properties of the $J^{PC} = 1^{-+}$ hybrid states. We have considered the normal decay process depicted in Fig. 5(a). We have also considered the abnormal decay processes depicted in Figs. 5(b) and 5(c), with the $\eta^{(\prime)}$

mesons produced by the QCD axial anomaly. The obtained results are summarized in Table III, and, especially,

$$\Gamma_{|\bar{q}qg;1^-1^{-+}\rangle} = 530^{+540}_{-330}\ \mathrm{MeV},$$
$$\Gamma_{|\bar{q}qg;0^+1^{-+}\rangle} = 120^{+160}_{-110}\ \mathrm{MeV},$$
$$\Gamma_{|\bar{s}sg;0^+1^{-+}\rangle} = 100^{+110}_{-80}\ \mathrm{MeV}.$$

The above QCD sum rule results suggest that the $\pi_1(1600)$ and $\eta_1(1855)$ can be, respectively, interpreted as the single-gluon hybrid states $|\bar{q}qg;1^-1^{-+}\rangle$ and $|\bar{s}sg;0^+1^{-+}\rangle$, so there exists another isoscalar state $|\bar{q}qg;0^+1^{-+}\rangle$, whose mass and width are smaller than those of $\eta_1(1855)$. Considering the uncertainties, our results suggest that the $\pi_1(1600)$ and $\eta_1(1855)$ may also be, respectively, interpreted as the single-gluon hybrid states $|\bar{q}qg;1^-1^{-+}\rangle$ and $|\bar{q}qg;0^+1^{-+}\rangle$, so there exists another isoscalar state $|\bar{s}sg;0^+1^{-+}\rangle$, whose mass and width are larger than those of $\eta_1(1855)$. To differentiate these two assignments, it is useful to examine the $a_1(1260)\pi$ decay channel. We find in Table III that the $\eta^{(\prime)}$-relevant decay modes, as the characteristic decay modes of hybrid states, are enhanced to some extent. To verify whether the exotic π_1 and η_1 resonances are hybrid states or not, we propose to examine these decay modes in future BESIII, Belle-II, GlueX, LHCb, and PANDA experiments.

ACKNOWLEDGMENTS

This project is supported by the National Natural Science Foundation of China under Grant No. 12075019, the Jiangsu Provincial Double-Innovation Program under Grant No. JSSCRC2021488, and the Fundamental Research Funds for the Central Universities.

APPENDIX: SPECTRAL DENSITIES

In this appendix, we show the OPE spectral densities extracted from the single-gluon hybrid currents given in Eqs. (7)–(14) and (19)–(30) with the quark-gluon content $\bar{s}sg$. Those with the quark-gluon content $\bar{q}qg$ $(q = u/d)$ can be easily derived by replacing $m_s \to 0$, $\langle\bar{s}s\rangle \to \langle\bar{q}q\rangle$, and $\langle g_s\bar{s}\sigma Gs\rangle \to \langle g_s\bar{q}\sigma Gq\rangle$:

$$\Pi^{\alpha\beta}_{1^{--}}(M_B^2,s_0) = \int_{4m_s^2}^{s_0}\left(\frac{s^3\alpha_s}{240\pi^3} - \frac{m_s^2 s^2\alpha_s}{24\pi^3} + s\left(\frac{\langle\alpha_s GG\rangle}{48\pi^2} - \frac{\langle\alpha_s GG\rangle\alpha_s}{1152\pi^3} - \frac{2m_s\langle\bar{s}s\rangle\alpha_s}{9\pi}\right) - \frac{\langle g_s^3G^3\rangle}{96\pi^2} - \frac{\langle\alpha_s GG\rangle m_s^2}{24\pi^2}\right) \times e^{-s/M_B^2}ds + \left(-\frac{\langle\alpha_s GG\rangle^2}{4608\pi^2} - \frac{\langle\alpha_s GG\rangle m_s\langle\bar{s}s\rangle}{18} - \frac{4}{9}m_s^2\pi\langle\bar{s}s\rangle^2\alpha_s + \frac{8}{9}\pi\langle\bar{s}s\rangle\langle g_s\bar{s}\sigma Gs\rangle\alpha_s\right), \tag{A1}$$

$$\tilde{\Pi}^{\alpha\beta}_{1^{+-}}(M_B^2,s_0) = \int_{4m_s^2}^{s_0}\left(\frac{s^3\alpha_s}{60\pi^3} - \frac{m_s^2 s^2\alpha_s}{6\pi^3} + s\left(-\frac{\langle\alpha_s GG\rangle}{12\pi^2} - \frac{\langle\alpha_s GG\rangle\alpha_s}{288\pi^3} - \frac{8m_s\langle\bar{s}s\rangle\alpha_s}{9\pi}\right) + \frac{\langle g_s^3G^3\rangle}{24\pi^2} + \frac{\langle\alpha_s GG\rangle m_s^2}{6\pi^2}\right) \times e^{-s/M_B^2}ds + \left(\frac{\langle\alpha_s GG\rangle^2}{1152\pi^2} - \frac{\langle g_s^3G^3\rangle m_s^2}{12\pi^2} + \frac{2}{9}\langle\alpha_s GG\rangle m_s\langle\bar{s}s\rangle - \frac{16}{9}\pi m_s^2\langle\bar{s}s\rangle^2\alpha_s + \frac{32}{9}\pi\langle\bar{s}s\rangle\langle g_s\bar{s}\sigma Gs\rangle\alpha_s\right), \tag{A2}$$

$$\Pi^{\alpha\beta}_{1^{+-}}(M_B^2,s_0) = \int_{4m_s^2}^{s_0}\left(\frac{s^3\alpha_s}{240\pi^3} - \frac{m_s^2 s^2\alpha_s}{8\pi^3} + s\left(\frac{\langle\alpha_s GG\rangle}{48\pi^2} - \frac{\langle\alpha_s GG\rangle\alpha_s}{1152\pi^3} + \frac{2m_s\langle\bar{s}s\rangle\alpha_s}{3\pi}\right) - \frac{\langle g_s^3G^3\rangle}{96\pi^2} - \frac{\langle\alpha_s GG\rangle m_s^2}{8\pi^2}\right) \times e^{-s/M_B^2}ds + \left(-\frac{\langle\alpha_s GG\rangle^2}{4608\pi^2} + \frac{\langle\alpha_s GG\rangle m_s\langle\bar{s}s\rangle}{6} - \frac{4}{9}m_s^2\pi\langle\bar{s}s\rangle^2\alpha_s - \frac{8}{9}\pi\langle\bar{s}s\rangle\langle g_s\bar{s}\sigma Gs\rangle\alpha_s\right), \tag{A3}$$

$$\tilde{\Pi}^{\alpha\beta}_{1^{--}}(M_B^2,s_0) = \int_{4m_s^2}^{s_0}\left(\frac{s^3\alpha_s}{60\pi^3} - \frac{m_s^2 s^2\alpha_s}{2\pi^3} + s\left(-\frac{\langle\alpha_s GG\rangle}{12\pi^2} - \frac{\langle\alpha_s GG\rangle\alpha_s}{288\pi^3} + \frac{8m_s\langle\bar{s}s\rangle\alpha_s}{3\pi}\right) + \frac{\langle g_s^3G^3\rangle}{24\pi^2} + \frac{\langle\alpha_s GG\rangle m_s^2}{2\pi^2}\right) \times e^{-s/M_B^2}ds + \left(\frac{\langle\alpha_s GG\rangle^2}{1152\pi^2} - \frac{\langle g_s^3G^3\rangle m_s^2}{4\pi^2} - \frac{2}{3}\langle\alpha_s GG\rangle m_s\langle\bar{s}s\rangle - \frac{16}{9}\pi m_s^2\langle\bar{s}s\rangle^2\alpha_s - \frac{32}{9}\pi\langle\bar{s}s\rangle\langle g_s\bar{s}\sigma Gs\rangle\alpha_s\right), \tag{A4}$$

$$\Pi^{\mu}_{1^{-+}}(M_B^2,s_0) = \int_{4m_s^2}^{s_0}\left(\frac{s^3\alpha_s}{60\pi^3} - \frac{m_s^2 s^2\alpha_s}{3\pi^3} + s\left(\frac{\langle\alpha_s GG\rangle}{36\pi^2} + \frac{13\langle\alpha_s GG\rangle\alpha_s}{432\pi^3} + \frac{8m_s\langle\bar{s}s\rangle\alpha_s}{9\pi}\right) + \frac{\langle g_s^3G^3\rangle}{32\pi^2} - \frac{3\langle\alpha_s GG\rangle m_s^2\alpha_s}{64\pi^3} - \frac{3m_s\langle g_s\bar{s}\sigma Gs\rangle\alpha_s}{4\pi}\right) \times e^{-s/M_B^2}ds + \left(\frac{\langle\alpha_s GG\rangle^2}{3456\pi^2} - \frac{\langle g_s^3G^3\rangle m_s^2}{16\pi^2} - \frac{2}{9}\langle\alpha_s GG\rangle m_s\langle\bar{s}s\rangle + \frac{11}{9}\pi\langle\bar{s}s\rangle\langle g_s\bar{s}\sigma Gs\rangle\alpha_s\right), \tag{A5}$$

$$\tilde{\Pi}^{\mu}_{1^{++}}(M_B^2,s_0) = \int_{4m_s^2}^{s_0}\left(\frac{s^3\alpha_s}{15\pi^3} - \frac{4m_s^2s^2\alpha_s}{3\pi^3} + s\left(-\frac{\langle\alpha_sGG\rangle}{9\pi^2} - \frac{5\langle\alpha_sGG\rangle\alpha_s}{108\pi^3} + \frac{32m_s\langle\bar{s}s\rangle\alpha_s}{9\pi}\right) - \frac{\langle g_s^3G^3\rangle}{4\pi^2} + \frac{3\langle\alpha_sGG\rangle m_s^2\alpha_s}{16\pi^3} + \frac{3m_s\langle g_s\bar{s}\sigma Gs\rangle\alpha_s}{\pi}\right)\times e^{-s/M_B^2}ds + \left(-\frac{\langle\alpha_sGG\rangle^2}{864\pi^2} + \frac{\langle g_s^3G^3\rangle m_s^2}{3\pi^2} + \frac{8}{9}\langle\alpha_sGG\rangle m_s\langle\bar{s}s\rangle - \frac{\langle\alpha_sGG\rangle m_s\langle\bar{s}s\rangle\alpha_s}{3\pi} - \frac{28}{9}\pi\langle\bar{s}s\rangle\langle g_s\bar{s}\sigma Gs\rangle\alpha_s\right), \tag{A6}$$

$$\Pi^{\mu}_{1^{+-}}(M_B^2,s_0) = \int_{4m_s^2}^{s_0}\left(\frac{s^3\alpha_s}{60\pi^3} - \frac{5m_s^2s^2\alpha_s}{12\pi^3} + s\left(\frac{\langle\alpha_sGG\rangle}{36\pi^2} + \frac{13\langle\alpha_sGG\rangle\alpha_s}{432\pi^3} + \frac{16m_s\langle\bar{s}s\rangle\alpha_s}{9\pi}\right) + \frac{\langle g_s^3G^3\rangle}{32\pi^2} - \frac{\langle\alpha_sGG\rangle m_s^2}{4\pi^2} - \frac{3\langle\alpha_sGG\rangle m_s^2\alpha_s}{64\pi^3} + \frac{3m_s\langle g_s\bar{s}\sigma Gs\rangle\alpha_s}{4\pi}\right)\times e^{-s/M_B^2}ds + \left(\frac{\langle\alpha_sGG\rangle^2}{3456\pi^2} - \frac{\langle g_s^3G^3\rangle m_s^2}{48\pi^2} + \frac{4}{9}\langle\alpha_sGG\rangle m_s\langle\bar{s}s\rangle - \frac{11}{9}\pi\langle\bar{s}s\rangle\langle g_s\bar{s}\sigma Gs\rangle\alpha_s\right), \tag{A7}$$

$$\tilde{\Pi}^{\mu}_{1^{--}}(M_B^2,s_0) = \int_{4m_s^2}^{s_0}\left(\frac{s^3\alpha_s}{15\pi^3} - \frac{5m_s^2s^2\alpha_s}{3\pi^3} + s\left(-\frac{\langle\alpha_sGG\rangle}{9\pi^2} - \frac{5\langle\alpha_sGG\rangle\alpha_s}{108\pi^3} + \frac{64m_s\langle\bar{s}s\rangle\alpha_s}{9\pi}\right) - \frac{\langle g_s^3G^3\rangle}{4\pi^2} + \frac{\langle\alpha_sGG\rangle m_s^2}{\pi^2} + \frac{3\langle\alpha_sGG\rangle m_s^2\alpha_s}{16\pi^3} - \frac{3m_s\langle g_s\bar{s}\sigma Gs\rangle\alpha_s}{\pi}\right)\times e^{-s/M_B^2}ds + \left(-\frac{\langle\alpha_sGG\rangle^2}{864\pi^2} - \frac{16}{9}\langle\alpha_sGG\rangle m_s\langle\bar{s}s\rangle - \frac{\langle\alpha_sGG\rangle m_s\langle\bar{s}s\rangle\alpha_s}{3\pi} + \frac{28}{9}\pi\langle\bar{s}s\rangle\langle g_s\bar{s}\sigma Gs\rangle\alpha_s\right), \tag{A8}$$

$$\Pi^{\mu}_{0^{++}}(M_B^2,s_0) = \int_{4m_s^2}^{s_0}\left(\frac{s^3\alpha_s}{120\pi^3} + s\left(-\frac{\langle\alpha_sGG\rangle}{24\pi^2} + \frac{\langle\alpha_sGG\rangle\alpha_s}{576\pi^3} - \frac{4m_s\langle\bar{s}s\rangle\alpha_s}{3\pi}\right) - \frac{3\langle g_s^3G^3\rangle}{32\pi^2} + \frac{\langle\alpha_sGG\rangle m_s^2}{12\pi^2} - \frac{3\langle\alpha_sGG\rangle m_s^2\alpha_s}{64\pi^3} + \frac{32}{9}\pi\langle\bar{s}s\rangle^2\alpha_s + \frac{13\langle g_s\bar{s}\sigma Gs\rangle m_s\alpha_s}{12\pi}\right)\times e^{-s/M_B^2}ds + \left(-\frac{\langle\alpha_sGG\rangle^2}{2304\pi^2} - \frac{\langle g_s^3G^3\rangle m_s^2}{16\pi^2} + \frac{1}{3}\langle\alpha_sGG\rangle m_s\langle\bar{s}s\rangle - \frac{\langle\alpha_sGG\rangle m_s\langle\bar{s}s\rangle\alpha_s}{8\pi} - \frac{8\pi m_s^2\langle\bar{s}s\rangle^2\alpha_s}{3} - \frac{1}{3}\pi\langle\bar{s}s\rangle\langle g_s\bar{s}\sigma Gs\rangle\alpha_s\right), \tag{A9}$$

$$\tilde{\Pi}^{\mu}_{0^{-+}}(M_B^2,s_0) = \int_{4m_s^2}^{s_0}\left(\frac{s^3\alpha_s}{30\pi^3} + s\left(\frac{\langle\alpha_sGG\rangle}{6\pi^2} + \frac{37\langle\alpha_sGG\rangle\alpha_s}{144\pi^3} - \frac{16m_s\langle\bar{s}s\rangle\alpha_s}{3\pi}\right) + \frac{\langle g_s^3G^3\rangle}{4\pi^2} - \frac{\langle\alpha_sGG\rangle m_s^2}{3\pi^2} - \frac{13\langle\alpha_sGG\rangle m_s^2\alpha_s}{16\pi^3} + \frac{128}{9}\pi\langle\bar{s}s\rangle^2\alpha_s - \frac{5\langle g_s\bar{s}\sigma Gs\rangle m_s\alpha_s}{3\pi}\right)\times e^{-s/M_B^2}ds + \left(\frac{\langle\alpha_sGG\rangle^2}{576\pi^2} - \frac{\langle g_s^3G^3\rangle m_s^2}{2\pi^2} - \frac{4}{3}\langle\alpha_sGG\rangle m_s\langle\bar{s}s\rangle - \frac{\langle\alpha_sGG\rangle m_s\langle\bar{s}s\rangle\alpha_s}{2\pi} - \frac{32\pi m_s^2\langle\bar{s}s\rangle^2\alpha_s}{3} + \frac{20}{3}\pi\langle\bar{s}s\rangle\langle g_s\bar{s}\sigma Gs\rangle\alpha_s\right), \tag{A10}$$

$$\Pi^{\mu}_{0^{--}}(M_B^2,s_0) = \int_{4m_s^2}^{s_0}\left(\frac{s^3\alpha_s}{120\pi^3} - \frac{m_s^2s^2\alpha_s}{4\pi^3} + s\left(-\frac{\langle\alpha_sGG\rangle}{24\pi^2} + \frac{\langle\alpha_sGG\rangle\alpha_s}{576\pi^3} + \frac{4m_s\langle\bar{s}s\rangle\alpha_s}{3\pi}\right) - \frac{3\langle g_s^3G^3\rangle}{32\pi^2} + \frac{\langle\alpha_sGG\rangle m_s^2}{3\pi^2} - \frac{3\langle\alpha_sGG\rangle m_s^2\alpha_s}{64\pi^3} - \frac{32}{9}\pi\langle\bar{s}s\rangle^2\alpha_s - \frac{13\langle g_s\bar{s}\sigma Gs\rangle m_s\alpha_s}{12\pi}\right)\times e^{-s/M_B^2}ds + \left(-\frac{\langle\alpha_sGG\rangle^2}{2304\pi^2} - \frac{3\langle g_s^3G^3\rangle m_s^2}{16\pi^2} - \frac{1}{3}\langle\alpha_sGG\rangle m_s\langle\bar{s}s\rangle - \frac{\langle\alpha_sGG\rangle m_s\langle\bar{s}s\rangle\alpha_s}{8\pi} - \frac{8\pi m_s^2\langle\bar{s}s\rangle^2\alpha_s}{3} + \frac{1}{3}\pi\langle\bar{s}s\rangle\langle g_s\bar{s}\sigma Gs\rangle\alpha_s\right), \tag{A11}$$

$$\tilde{\Pi}^{\mu}_{0^{+-}}(M_B^2,s_0) = \int_{4m_s^2}^{s_0}\left(\frac{s^3\alpha_s}{30\pi^3} - \frac{m_s^2s^2\alpha_s}{\pi^3} + s\left(+\frac{\langle\alpha_sGG\rangle}{6\pi^2} + \frac{37\langle\alpha_sGG\rangle\alpha_s}{144\pi^3} + \frac{16m_s\langle\bar{s}s\rangle\alpha_s}{3\pi}\right) + \frac{\langle g_s^3G^3\rangle}{4\pi^2} - \frac{4\langle\alpha_sGG\rangle m_s^2}{3\pi^2} - \frac{13\langle\alpha_sGG\rangle m_s^2\alpha_s}{16\pi^3} - \frac{128}{9}\pi\langle\bar{s}s\rangle^2\alpha_s + \frac{5\langle g_s\bar{s}\sigma Gs\rangle m_s\alpha_s}{3\pi}\right)\times e^{-s/M_B^2}ds + \left(\frac{\langle\alpha_sGG\rangle^2}{576\pi^2} - \frac{\langle g_s^3G^3\rangle m_s^2}{2\pi^2} + \frac{4}{3}\langle\alpha_sGG\rangle m_s\langle\bar{s}s\rangle - \frac{\langle\alpha_sGG\rangle m_s\langle\bar{s}s\rangle\alpha_s}{2\pi} - \frac{32\pi m_s^2\langle\bar{s}s\rangle^2\alpha_s}{3} - \frac{20}{3}\pi\langle\bar{s}s\rangle\langle g_s\bar{s}\sigma Gs\rangle\alpha_s\right), \tag{A12}$$

$$\Pi_{0^{++}}(M_B^2,s_0)=\int_{4m_s^2}^{s_0}\left(\frac{s^3\alpha_s}{6\pi^3}-\frac{4m_s^2s^2\alpha_s}{\pi^3}+s\left(\frac{37\langle\alpha_sGG\rangle\alpha_s}{48\pi^3}+\frac{16m_s\langle\bar{s}s\rangle\alpha_s}{\pi}\right)-\frac{\langle g_s^3G^3\rangle}{4\pi^2}-\frac{\langle\alpha_sGG\rangle m_s^2}{\pi^2}-\frac{3\langle\alpha_sGG\rangle m_s^2\alpha_s}{2\pi^3}\right.$$
$$\left.+\frac{12m_s\langle g_s\bar{s}\sigma Gs\rangle\alpha_s}{\pi}\right)\times e^{-s/M_B^2}ds+\left(\frac{3\langle g_s^3G^3\rangle m_s^2}{4\pi^2}+\frac{8}{3}\langle\alpha_sGG\rangle m_s\langle\bar{s}s\rangle+\frac{\langle\alpha_sGG\rangle m_s\langle\bar{s}s\rangle\alpha_s}{\pi}\right.$$
$$\left.+\frac{32\pi m_s^2\langle\bar{s}s\rangle^2\alpha_s}{3}-16\pi\langle\bar{s}s\rangle\langle g_s\bar{s}\sigma Gs\rangle\alpha_s\right),\qquad\text{(A13)}$$

$$\Pi_{0^{-+}}(M_B^2,s_0)=\int_{4m_s^2}^{s_0}\left(\frac{s^3\alpha_s}{6\pi^3}-\frac{4m_s^2s^2\alpha_s}{\pi^3}+s\left(\frac{37\langle\alpha_sGG\rangle\alpha_s}{48\pi^3}+\frac{16m_s\langle\bar{s}s\rangle\alpha_s}{\pi}\right)-\frac{\langle g_s^3G^3\rangle}{4\pi^2}+\frac{\langle\alpha_sGG\rangle m_s^2}{\pi^2}-\frac{3\langle\alpha_sGG\rangle m_s^2\alpha_s}{2\pi^3}\right.$$
$$\left.-\frac{12m_s\langle g_s\bar{s}\sigma Gs\rangle\alpha_s}{\pi}\right)\times e^{-s/M_B^2}ds+\left(\frac{\langle g_s^3G^3\rangle m_s^2}{4\pi^2}-\frac{8}{3}\langle\alpha_sGG\rangle m_s\langle\bar{s}s\rangle+\frac{\langle\alpha_sGG\rangle m_s\langle\bar{s}s\rangle\alpha_s}{\pi}+\frac{32\pi m_s^2\langle\bar{s}s\rangle^2\alpha_s}{3}\right.$$
$$\left.+16\pi\langle\bar{s}s\rangle\langle g_s\bar{s}\sigma Gs\rangle\alpha_s\right),\qquad\text{(A14)}$$

$$\Pi_{1^{++}}^{\alpha\beta}(M_B^2,s_0)=\int_{4m_s^2}^{s_0}\left(\frac{s^3\alpha_s}{60\pi^3}-\frac{m_s^2s^2\alpha_s}{3\pi^3}+s\left(\frac{19\langle\alpha_sGG\rangle\alpha_s}{864\pi^3}+\frac{8m_s\langle\bar{s}s\rangle\alpha_s}{9\pi}\right)-\frac{\langle\alpha_sGG\rangle m_s^2}{6\pi^2}+\frac{m_s\langle g_s\bar{s}\sigma Gs\rangle\alpha_s}{\pi}\right)\times e^{-s/M_B^2}ds$$
$$+\left(-\frac{\langle g_s^3G^3\rangle m_s^2}{24\pi^2}+\frac{4}{9}\langle\alpha_sGG\rangle m_s\langle\bar{s}s\rangle-\frac{\langle\alpha_sGG\rangle m_s\langle\bar{s}s\rangle\alpha_s}{12\pi}-\frac{16\pi m_s^2\langle\bar{s}s\rangle^2\alpha_s}{9}-\frac{4}{3}\pi\langle\bar{s}s\rangle\langle g_s\bar{s}\sigma Gs\rangle\alpha_s\right),\qquad\text{(A15)}$$

$$\tilde{\Pi}_{1^{-+}}^{\alpha\beta}(M_B^2,s_0)=\int_{4m_s^2}^{s_0}\left(\frac{s^3\alpha_s}{15\pi^3}-\frac{4m_s^2s^2\alpha_s}{3\pi^3}+s\left(\frac{19\langle\alpha_sGG\rangle\alpha_s}{216\pi^3}+\frac{32m_s\langle\bar{s}s\rangle\alpha_s}{9\pi}\right)+\frac{2\langle\alpha_sGG\rangle m_s^2}{3\pi^2}-\frac{4m_s\langle g_s\bar{s}\sigma Gs\rangle\alpha_s}{\pi}\right)\times e^{-s/M_B^2}ds$$
$$+\left(-\frac{\langle g_s^3G^3\rangle m_s^2}{2\pi^2}-\frac{16}{9}\langle\alpha_sGG\rangle m_s\langle\bar{s}s\rangle-\frac{\langle\alpha_sGG\rangle m_s\langle\bar{s}s\rangle\alpha_s}{3\pi}-\frac{64\pi m_s^2\langle\bar{s}s\rangle^2\alpha_s}{9}+\frac{16}{3}\pi\langle\bar{s}s\rangle\langle g_s\bar{s}\sigma Gs\rangle\alpha_s\right),\qquad\text{(A16)}$$

$$\Pi_{1^{-+}}^{\alpha\beta}(M_B^2,s_0)=\int_{4m_s^2}^{s_0}\left(\frac{s^3\alpha_s}{60\pi^3}-\frac{m_s^2s^2\alpha_s}{3\pi^3}+s\left(\frac{19\langle\alpha_sGG\rangle\alpha_s}{864\pi^3}+\frac{8m_s\langle\bar{s}s\rangle\alpha_s}{9\pi}\right)+\frac{\langle\alpha_sGG\rangle m_s^2}{6\pi^2}-\frac{m_s\langle g_s\bar{s}\sigma Gs\rangle\alpha_s}{\pi}\right)\times e^{-s/M_B^2}ds$$
$$+\left(-\frac{\langle g_s^3G^3\rangle m_s^2}{8\pi^2}-\frac{4}{9}\langle\alpha_sGG\rangle m_s\langle\bar{s}s\rangle-\frac{\langle\alpha_sGG\rangle m_s\langle\bar{s}s\rangle\alpha_s}{12\pi}-\frac{16\pi m_s^2\langle\bar{s}s\rangle^2\alpha_s}{9}+\frac{4}{3}\pi\langle\bar{s}s\rangle\langle g_s\bar{s}\sigma Gs\rangle\alpha_s\right),\qquad\text{(A17)}$$

$$\tilde{\Pi}_{1^{++}}^{\alpha\beta}(M_B^2,s_0)=\int_{4m_s^2}^{s_0}\left(\frac{s^3\alpha_s}{15\pi^3}-\frac{4m_s^2s^2\alpha_s}{3\pi^3}+s\left(\frac{19\langle\alpha_sGG\rangle\alpha_s}{216\pi^3}+\frac{32m_s\langle\bar{s}s\rangle\alpha_s}{9\pi}\right)-\frac{2\langle\alpha_sGG\rangle m_s^2}{3\pi^2}+\frac{4m_s\langle g_s\bar{s}\sigma Gs\rangle\alpha_s}{\pi}\right)\times e^{-s/M_B^2}ds$$
$$+\left(-\frac{\langle g_s^3G^3\rangle m_s^2}{6\pi^2}+\frac{16}{9}\langle\alpha_sGG\rangle m_s\langle\bar{s}s\rangle-\frac{\langle\alpha_sGG\rangle m_s\langle\bar{s}s\rangle\alpha_s}{3\pi}-\frac{64\pi m_s^2\langle\bar{s}s\rangle^2\alpha_s}{9}-\frac{16}{3}\pi\langle\bar{s}s\rangle\langle g_s\bar{s}\sigma Gs\rangle\alpha_s\right),\qquad\text{(A18)}$$

$$\Pi_{2^{++}}^{\alpha_1\beta_1,\alpha_2\beta_2}(M_B^2,s_0)=\int_{4m_s^2}^{s_0}\left(\frac{2s^3\alpha_s}{15\pi^3}-\frac{22m_s^2s^2\alpha_s}{5\pi^3}+s\left(\frac{\langle\alpha_sGG\rangle}{3\pi^2}-\frac{89\langle\alpha_sGG\rangle\alpha_s}{144\pi^3}+\frac{80m_s\langle\bar{s}s\rangle\alpha_s}{3\pi}\right)-\frac{2\langle\alpha_sGG\rangle m_s^2}{\pi^2}\right.$$
$$\left.-\frac{12m_s\langle g_s\bar{s}\sigma Gs\rangle\alpha_s}{\pi}\right)\times e^{-s/M_B^2}ds+\left(-\frac{\langle\alpha_sGG\rangle^2}{288\pi^2}-\frac{3\langle g_s^3G^3\rangle m_s^2}{\pi^2}+\frac{8}{3}\langle\alpha_sGG\rangle m_s\langle\bar{s}s\rangle\right.$$
$$\left.+\frac{2\langle\alpha_sGG\rangle m_s\langle\bar{s}s\rangle\alpha_s}{\pi}-\frac{176}{3}\pi\langle\bar{s}s\rangle\langle g_s\bar{s}\sigma Gs\rangle\alpha_s\right),\qquad\text{(A19)}$$

$$\tilde{\Pi}_{2^{-+}}^{\alpha_1\beta_1,\alpha_2\beta_2}(M_B^2,s_0)=\int_{4m_s^2}^{s_0}\left(\frac{8s^3\alpha_s}{15\pi^3}-\frac{88m_s^2s^2\alpha_s}{5\pi^3}+s\left(-\frac{4\langle\alpha_sGG\rangle}{3\pi^2}-\frac{17\langle\alpha_sGG\rangle\alpha_s}{36\pi^3}+\frac{320m_s\langle\bar{s}s\rangle\alpha_s}{3\pi}\right)+\frac{8\langle\alpha_sGG\rangle m_s^2}{\pi^2}\right.$$
$$\left.+\frac{48m_s\langle g_s\bar{s}\sigma Gs\rangle\alpha_s}{\pi}\right)\times e^{-s/M_B^2}ds+\left(\frac{\langle\alpha_sGG\rangle^2}{72\pi^2}+\frac{8\langle g_s^3G^3\rangle m_s^2}{\pi^2}-\frac{32}{3}\langle\alpha_sGG\rangle m_s\langle\bar{s}s\rangle\right.$$
$$\left.-\frac{1088}{3}\pi\langle\bar{s}s\rangle\langle g_s\bar{s}\sigma Gs\rangle\alpha_s\right),\qquad\text{(A20)}$$

$$\Pi_{2^{-+}}^{\alpha_1\beta_1,\alpha_2\beta_2}(M_B^2,s_0) = \int_{4m_s^2}^{s_0}\left(\frac{2s^3\alpha_s}{15\pi^3} - \frac{2m_s^2s^2\alpha_s}{5\pi^3} + s\left(\frac{\langle\alpha_s GG\rangle}{3\pi^2} - \frac{89\langle\alpha_s GG\rangle\alpha_s}{144\pi^3} - \frac{16m_s\langle\bar{s}s\rangle\alpha_s}{\pi}\right) + \frac{2\langle\alpha_s GG\rangle m_s^2}{\pi^2} + \frac{12m_s\langle g_s\bar{s}\sigma Gs\rangle\alpha_s}{\pi}\right)\times e^{-s/M_B^2}ds + \left(-\frac{\langle\alpha_s GG\rangle^2}{288\pi^2} - \frac{3\langle g_s^3G^3\rangle m_s^2}{\pi^2} - 8\langle\alpha_s GG\rangle m_s\langle\bar{s}s\rangle + \frac{2\langle\alpha_s GG\rangle m_s\langle\bar{s}s\rangle\alpha_s}{\pi} + \frac{176}{3}\pi\langle\bar{s}s\rangle\langle g_s\bar{s}\sigma Gs\rangle\alpha_s\right), \tag{A21}$$

$$\tilde{\Pi}_{2^{++}}^{\alpha_1\beta_1,\alpha_2\beta_2}(M_B^2,s_0) = \int_{4m_s^2}^{s_0}\left(\frac{8s^3\alpha_s}{15\pi^3} - \frac{8m_s^2s^2\alpha_s}{5\pi^3} + s\left(-\frac{4\langle\alpha_s GG\rangle}{3\pi^2} - \frac{17\langle\alpha_s GG\rangle\alpha_s}{36\pi^3} - \frac{64m_s\langle\bar{s}s\rangle\alpha_s}{\pi}\right) - \frac{8\langle\alpha_s GG\rangle m_s^2}{\pi^2} - \frac{48m_s\langle g_s\bar{s}\sigma Gs\rangle\alpha_s}{\pi}\right)\times e^{-s/M_B^2}ds + \left(\frac{\langle\alpha_s GG\rangle^2}{72\pi^2} + \frac{16\langle g_s^3G^3\rangle m_s^2}{\pi^2} + 32\langle\alpha_s GG\rangle m_s\langle\bar{s}s\rangle + \frac{1088}{3}\pi\langle\bar{s}s\rangle\langle g_s\bar{s}\sigma Gs\rangle\alpha_s\right). \tag{A22}$$

[1] P. A. Zyla *et al.*, Review of particle physics, Prog. Theor. Exp. Phys. **2020**, 083C01 (2020).
[2] E. Klempt and A. Zaitsev, Glueballs, hybrids, multiquarks: Experimental facts versus QCD inspired concepts, Phys. Rep. **454**, 1 (2007).
[3] C. Amsler and N. A. Tornqvist, Mesons beyond the naive quark model, Phys. Rep. **389**, 61 (2004).
[4] D. V. Bugg, Four sorts of meson, Phys. Rep. **397**, 257 (2004).
[5] C. A. Meyer and Y. Van Haarlem, Status of exotic-quantum-number mesons, Phys. Rev. C **82**, 025208 (2010).
[6] C. A. Meyer and E. S. Swanson, Hybrid mesons, Prog. Part. Nucl. Phys. **82**, 21 (2015).
[7] H.-X. Chen, W. Chen, X. Liu, and S.-L. Zhu, The hidden-charm pentaquark and tetraquark states, Phys. Rep. **639**, 1 (2016).
[8] R. A. Briceno, J. J. Dudek, and R. D. Young, Scattering processes and resonances from lattice QCD, Rev. Mod. Phys. **90**, 025001 (2018).
[9] B. Ketzer, B. Grube, and D. Ryabchikov, Light-meson spectroscopy with COMPASS, Prog. Part. Nucl. Phys. **113**, 103755 (2020).
[10] S. Jin and X. Shen, Highlights of light meson spectroscopy at the BESIII experiment, Natl. Sci. Rev. **8**, nwab198 (2021).
[11] H.-X. Chen, W. Chen, X. Liu, Y.-R. Liu, and S.-L. Zhu, An updated review of the new hadron states, Rep. Prog. Phys. **86**, 026201 (2023).
[12] M. Ablikim *et al.*, Observation of an isoscalar resonance with exotic $J^{PC} = 1^{-+}$ quantum numbers in $J/\psi \to \gamma\eta\eta'$, Phys. Rev. Lett. **129**, 192002 (2022).
[13] M. Ablikim *et al.*, Partial wave analysis of $J/\psi \to \gamma\eta\eta'$, Phys. Rev. D **106**, 072012 (2022); **107**, 079901(E) (2023).
[14] D. Alde *et al.*, Evidence for a 1^{-+} exotic meson, Phys. Lett. B **205**, 397 (1988).
[15] G. S. Adams *et al.*, Observation of a new $J^{PC} = 1^{-+}$ exotic state in the reaction $\pi^- p \to \pi^+\pi^-\pi^- p$ at 18 GeV$/c$, Phys. Rev. Lett. **81**, 5760 (1998).
[16] J. Kuhn *et al.*, Exotic meson production in the $f_1(1285)\pi^-$ system observed in the reaction $\pi^- p \to \eta\pi^+\pi^-\pi^- p$ at 18 GeV$/c$, Phys. Lett. B **595**, 109 (2004).
[17] H. Aoyagi *et al.*, Study of the $\eta\pi^-$ system in the $\pi^- p$ reaction at 6.3 GeV$/c$, Phys. Lett. B **314**, 246 (1993).
[18] D. R. Thompson *et al.*, Evidence for exotic meson production in the reaction $\pi^- p \to \eta\pi^- p$ at 18 GeV$/c$, Phys. Rev. Lett. **79**, 1630 (1997).
[19] V. Dorofeev (VES Collaboration), The $J^{PC} = 1^{-+}$ hunting season at VES, AIP Conf. Proc. **619**, 143 (2002).
[20] A. Abele *et al.*, Exotic $\eta\pi$ state in $\bar{p}d$ annihilation at rest into $\pi^-\pi^0\eta p_{\text{spectator}}$, Phys. Lett. B **423**, 175 (1998).
[21] M. Albrecht *et al.*, Coupled channel analysis of $\bar{p}p \to \pi^0\pi^0\eta$, $\pi^0\eta\eta$ and $K^+K^-\pi^0$ at 900 MeV/c and of $\pi\pi$-scattering data, Eur. Phys. J. C **80**, 453 (2020).
[22] The OBELIX Collaboration, $\bar{p}p$ annihilation into four charged pions at rest and in flight, Eur. Phys. J. C **35**, 21 (2004).
[23] M. Aghasyan *et al.*, Light isovector resonances in $\pi^- p \to \pi^-\pi^-\pi^+ p$ at 190 GeV$/c$, Phys. Rev. D **98**, 092003 (2018).
[24] Y. A. Khokhlov, Study of $X(1600)1^{-+}$ hybrid, Nucl. Phys. **A663**, 596 (2000).
[25] C. A. Baker *et al.*, Confirmation of $a_0(1450)$ and $\pi_1(1600)$ in $\bar{p}p \to \omega\pi^+\pi^-\pi^0$ at rest, Phys. Lett. B **563**, 140 (2003).
[26] M. Alekseev *et al.*, Observation of a $J^{PC} = 1^{-+}$ exotic resonance in diffractive dissociation of 190 GeV$/c$ π^- into $\pi^-\pi^-\pi^+$, Phys. Rev. Lett. **104**, 241803 (2010).

[27] G. S. Adams *et al.*, Amplitude analyses of the decays $\chi_{c1} \to \eta\pi^+\pi^-$ and $\chi_{c1} \to \eta'\pi^+\pi^-$, Phys. Rev. D **84**, 112009 (2011).
[28] M. Lu *et al.*, Exotic meson decay to $\omega\pi^0\pi^-$, Phys. Rev. Lett. **94**, 032002 (2005).
[29] C. Adolph *et al.*, Odd and even partial waves of $\eta\pi^-$ and $\eta'\pi^-$ in $\pi^- p \to \eta^{(\prime)}\pi^- p$ at 191 GeV$/c$, Phys. Lett. B **740**, 303 (2015).
[30] A. Rodas *et al.*, Determination of the pole position of the lightest hybrid meson candidate, Phys. Rev. Lett. **122**, 042002 (2019).
[31] G. D. Alexeev *et al.*, Exotic meson $\pi_1(1600)$ with $J^{PC} = 1^{-+}$ and its decay into $\rho(770)\pi$, Phys. Rev. D **105**, 012005 (2022).
[32] T. Barnes, Coloured quark and gluon constituents in the MIT bag model: A model of mesons, Nucl. Phys. **B158**, 171 (1979).
[33] P. Hasenfratz, R. R. Horgan, J. Kuti, and J. M. Richard, The effects of coloured glue in the QCD motivated bag of heavy quark-antiquark systems, Phys. Lett. **95B**, 299 (1980).
[34] M. S. Chanowitz and S. R. Sharpe, Hybrids: Mixed states of quarks and gluons, Nucl. Phys. **B222**, 211 (1983); **B228**, 588(E) (1983).
[35] N. Isgur and J. E. Paton, A flux tube model for hadrons, Phys. Lett. **124B**, 247 (1983).
[36] F. E. Close and P. R. Page, The production and decay of hybrid mesons by flux-tube breaking, Nucl. Phys. **B443**, 233 (1995).
[37] P. R. Page, E. S. Swanson, and A. P. Szczepaniak, Hybrid meson decay phenomenology, Phys. Rev. D **59**, 034016 (1999).
[38] L. Qiu and Q. Zhao, Towards the establishment of the light $J^{P(C)} = 1^{-(+)}$ hybrid nonet, Chin. Phys. C **46**, 051001 (2022).
[39] O. Andreev, Exotic hybrid pseudopotentials and gauge/string duality, Phys. Rev. D **87**, 065006 (2013).
[40] L. Bellantuono, P. Colangelo, and F. Giannuzzi, Exotic $J^{PC} = 1^{-+}$ mesons in a holographic model of QCD, Eur. Phys. J. C **74**, 2830 (2014).
[41] C. Michael, Adjoint sources in lattice gauge theory, Nucl. Phys. **B259**, 58 (1985).
[42] K. J. Juge, J. Kuti, and C. Morningstar, Fine structure of the QCD string spectrum, Phys. Rev. Lett. **90**, 161601 (2003).
[43] P. Lacock, C. Michael, P. Boyle, and P. Rowland, Hybrid mesons from quenched QCD, Phys. Lett. B **401**, 308 (1997).
[44] C. W. Bernard *et al.*, Exotic mesons in quenched lattice QCD, Phys. Rev. D **56**, 7039 (1997).
[45] J. J. Dudek, R. G. Edwards, P. Guo, and C. E. Thomas, Toward the excited isoscalar meson spectrum from lattice QCD, Phys. Rev. D **88**, 094505 (2013).
[46] L. J. Reinders, H. R. Rubinstein, and S. Yazaki, Hadron couplings to Goldstone bosons in QCD, Nucl. Phys. **B213**, 109 (1983).
[47] I. I. Balitsky, D. Diakonov, and A. V. Yung, Exotic mesons with $J^{PC} = 1^{-+}$ from QCD sum rules, Phys. Lett. **112B**, 71 (1982).
[48] J. Govaerts, F. de Viron, D. Gusbin, and J. Weyers, Exotic mesons from QCD sum rules, Phys. Lett. **128B**, 262 (1983); **136B**, 445(E) (1984).
[49] L. S. Kisslinger and Z. P. Li, Hybrid baryons via QCD sum rules, Phys. Rev. D **51**, R5986 (1995).
[50] H. Y. Jin, J. G. Korner, and T. G. Steele, Improved determination of the mass of the 1^{-+} light hybrid meson from QCD sum rules, Phys. Rev. D **67**, 014025 (2003).
[51] S.-H. Li, Z.-S. Chen, H.-Y. Jin, and W. Chen, Mass of 1^{-+} fourquark-hybrid mixed states, Phys. Rev. D **105**, 054030 (2022).
[52] D. Horn and J. Mandula, Model of mesons with constituent gluons, Phys. Rev. D **17**, 898 (1978).
[53] A. P. Szczepaniak and E. S. Swanson, Coulomb gauge QCD, confinement, and the constituent representation, Phys. Rev. D **65**, 025012 (2001).
[54] P. Guo, A. P. Szczepaniak, G. Galata, A. Vassallo, and E. Santopinto, Gluelump spectrum from Coulomb gauge QCD, Phys. Rev. D **77**, 056005 (2008).
[55] J. J. Coyne, P. M. Fishbane, and S. Meshkov, Glueballs: Their spectra, production and decay, Phys. Lett. **91B**, 259 (1980).
[56] M. S. Chanowitz, Have we seen our first glueball?, Phys. Rev. Lett. **46**, 981 (1981).
[57] T. Barnes, A transverse gluonium potential model with Breit-Fermi hyperfine effects, Z. Phys. C **10**, 275 (1981).
[58] J. M. Cornwall and A. Soni, Glueballs as bound states of massive gluons, Phys. Lett. **120B**, 431 (1983).
[59] Y. M. Cho, X. Y. Pham, P. Zhang, J.-J. Xie, and L.-P. Zou, Glueball physics in QCD, Phys. Rev. D **91**, 114020 (2015).
[60] D. Ebert, R. N. Faustov, and V. O. Galkin, Mass spectra and Regge trajectories of light mesons in the relativistic quark model, Phys. Rev. D **79**, 114029 (2009).
[61] H.-C. Kim and Y. Kim, Hybrid exotic meson with $J^{PC} = 1^{-+}$ in AdS/QCD, J. High Energy Phys. 01 (2009) 034.
[62] J. Ping, C. Deng, and F. Wang, Multiquark exotics study, Int. J. Mod. Phys. E **18**, 315 (2009).
[63] T. Kitazoe, M. Wada, M. Oka, M. Kawaguchi, and T. Morii, Spectroscopy of $Q\bar{Q}g$ hybrid mesons, Z. Phys. C **24**, 143 (1984).
[64] J. J. Dudek, R. G. Edwards, M. J. Peardon, D. G. Richards, and C. E. Thomas, Toward the excited meson spectrum of dynamical QCD, Phys. Rev. D **82**, 034508 (2010).
[65] J. J. Dudek, R. G. Edwards, M. J. Peardon, D. G. Richards, and C. E. Thomas, Highly excited and exotic meson spectrum from dynamical lattice QCD, Phys. Rev. Lett. **103**, 262001 (2009).
[66] L. S. Kisslinger, Mixed heavy quark hybrid mesons, decay puzzles, and RHIC, Phys. Rev. D **79**, 114026 (2009).
[67] J. N. Hedditch, W. Kamleh, B. G. Lasscock, D. B. Leinweber, A. G. Williams, and J. M. Zanotti, 1^{-+} exotic meson at light quark masses, Phys. Rev. D **72**, 114507 (2005).
[68] C. Bernard, T. Burch, E. B. Gregory, D. Toussaint, C. E. DeTar, J. Osborn, S. A. Gottlieb, U. M. Heller, and R. Sugar, Lattice calculation of 1^{-+} hybrid mesons with improved Kogut-Susskind fermions, Phys. Rev. D **68**, 074505 (2003).

[69] C. McNeile, C. W. Bernard, T. A. DeGrand, C. E. DeTar, S. A. Gottlieb, U. M. Heller, J. Hetrick, R. Sugar, and D. Toussaint, Exotic meson spectroscopy from the clover action at $\beta = 5.85$ and $\beta = 6.15$, Nucl. Phys. B, Proc. Suppl. **73**, 264 (1999).
[70] N. Isgur and J. E. Paton, Flux-tube model for hadrons in QCD, Phys. Rev. D **31**, 2910 (1985).
[71] T. Burns and F. E. Close, Hybrid-meson properties in lattice QCD and flux-tube models, Phys. Rev. D **74**, 034003 (2006).
[72] F. Iddir and L. Semlala, Hybrid states from constituent glue model, Int. J. Mod. Phys. A **23**, 5229 (2008).
[73] J. Govaerts, F. de Viron, D. Gusbin, and J. Weyers, QCD sum rules and hybrid mesons, Nucl. Phys. **B248**, 1 (1984).
[74] K. G. Chetyrkin and S. Narison, Light hybrid mesons in QCD, Phys. Lett. B **485**, 145 (2000).
[75] T. Huang, H.-y. Jin, and A.-l. Zhang, The masses of the 0^{++} and 0^{-+} light-quark hybrids using QCD sum rules, Eur. Phys. J. C **8**, 465 (1999).
[76] J. I. Latorre, P. Pascual, and S. Narison, Spectra and hadronic couplings of light hermaphrodite mesons, Z. Phys. C **34**, 347 (1987).
[77] K.-C. Yang, Indications of the possible observation of the lowest-lying 1^{-+} QCD state, Phys. Rev. D **76**, 094001 (2007).
[78] L. J. Reinders, S. Yazaki, and H. R. Rubinstein, $L = 1$ light quark mesons in QCD, Nucl. Phys. **B196**, 125 (1982).
[79] S. Narison, 1^{-+} light exotic mesons in QCD, Phys. Lett. B **675**, 319 (2009).
[80] J. Ho, R. Berg, W. Chen, D. Harnett, and T. G. Steele, Mass calculations of light quarkonium, exotic $J^{PC} = 0^{+-}$ hybrid mesons from Gaussian sum rules, Phys. Rev. D **98**, 096020 (2018).
[81] Q.-N. Wang, D.-K. Lian, and W. Chen, Predictions of the hybrid mesons with exotic quantum numbers $J^{PC} = 2^{+-}$, Phys. Rev. D **108**, 114010 (2023).
[82] P. R. Page, Why hybrid meson coupling to two S-wave mesons is suppressed, Phys. Lett. B **402**, 183 (1997).
[83] N. Isgur, R. Kokoski, and J. Paton, Gluonic excitations of mesons: Why they are missing and where to find them, Phys. Rev. Lett. **54**, 869 (1985).
[84] F. De Viron and J. Govaerts, Some decay modes of 1^{-+} hybrid mesons, Phys. Rev. Lett. **53**, 2207 (1984).
[85] J. M. Frere and S. Titard, A new look at exotic decays: $\tilde{\rho}(1^{-+}, I = 1) \to \eta'\pi$ versus $\rho\pi$, Phys. Lett. B **214**, 463 (1988).
[86] S.-L. Zhu, Masses and decay widths of heavy hybrid mesons, Phys. Rev. D **60**, 014008 (1999).
[87] S.-L. Zhu, Some decay modes of the 1^{-+} hybrid meson in QCD sum rules revisited, Phys. Rev. D **60**, 097502 (1999).
[88] S. Godfrey and J. L. Rosner, Production of singlet P-wave $c\bar{c}$ and $b\bar{b}$ states, Phys. Rev. D **66**, 014012 (2002).
[89] C. McNeile and C. Michael, Decay width of light quark hybrid meson from the lattice, Phys. Rev. D **73**, 074506 (2006).
[90] A.-l. Zhang and T. G. Steele, Decays of the $\hat{\rho}(1^{-+})$ exotic hybrid and $\eta - \eta'$ mixing, Phys. Rev. D **65**, 114013 (2002).
[91] F. E. Close and P. R. Page, Photoproduction of hybrid mesons from CEBAF to DESY HERA, Phys. Rev. D **52**, 1706 (1995).
[92] A. Afanasev and P. R. Page, Photoproduction and electroproduction of $J^{PC} = 1^{-+}$ exotics, Phys. Rev. D **57**, 6771 (1998).
[93] A. P. Szczepaniak and M. Swat, Role of photoproduction in exotic meson searches, Phys. Lett. B **516**, 72 (2001).
[94] V. Shastry, C. S. Fischer, and F. Giacosa, The phenomenology of the exotic hybrid nonet with $\pi_1(1600)$ and $\eta_1(1855)$, Phys. Lett. B **834**, 137478 (2022).
[95] F. Chen, X. Jiang, Y. Chen, M. Gong, Z. Liu, C. Shi, and W. Sun, 1^{-+} hybrid meson in J/ψ radiative decays from lattice QCD, Phys. Rev. D **107**, 054511 (2023).
[96] Y. Yu, Z. Xiong, H. Zhang, B.-C. Ke, Y. Teng, Q.-S. Liu, and J.-W. Zhang, Investigating the $\eta_1'(1855)$ exotic state in the $J/\psi \to \eta_1'(1855)\eta^{(\prime)}$ decays, Phys. Lett. B **842**, 137965 (2023).
[97] H.-X. Chen, A. Hosaka, and S.-L. Zhu, $I^G J^{PC} = 0^+1^{-+}$ tetraquark states, Phys. Rev. D **78**, 117502 (2008).
[98] H.-X. Chen, A. Hosaka, and S.-L. Zhu, $I^G J^{PC} = 1^-1^{-+}$ tetraquark states, Phys. Rev. D **78**, 054017 (2008).
[99] H.-X. Chen, W. Chen, X. Liu, T. G. Steele, and S.-L. Zhu, Towards exotic hidden-charm pentaquarks in QCD, Phys. Rev. Lett. **115**, 172001 (2015).
[100] X. Zhang and J.-J. Xie, Prediction of possible exotic states in the $\eta\bar{K}K^*$ system, Chin. Phys. C **44**, 054104 (2020).
[101] C.-M. Tang, Y.-C. Zhao, and L. Tang, Mass predictions of vector (1^{--}) double-gluon heavy quarkonium hybrids from QCD sum rules, Phys. Rev. D **105**, 114004 (2022).
[102] X.-K. Dong, Y.-H. Lin, and B.-S. Zou, Interpretation of the $\eta_1(1855)$ as a $K\bar{K}_1(1400)$ + c.c. molecule, Sci. China Phys. Mech. Astron. **65**, 261011 (2022).
[103] F. Yang, H. Q. Zhu, and Y. Huang, Analysis of the $\eta_1(1855)$ as a $K\bar{K}_1(1400)$ molecular state, Nucl. Phys. **A1030**, 122571 (2023).
[104] B.-D. Wan, S.-Q. Zhang, and C.-F. Qiao, Possible structure of the newly found exotic state $\eta_1(1855)$, Phys. Rev. D **106**, 074003 (2022).
[105] X.-Y. Wang, F.-C. Zeng, and X. Liu, Production of the $\eta_1(1855)$ through kaon induced reactions under the assumptions that it is a molecular or a hybrid state, Phys. Rev. D **106**, 036005 (2022).
[106] T. Ji, X.-K. Dong, F.-K. Guo, and B.-S. Zou, Prediction of a narrow exotic hadronic state with quantum numbers $J^{PC} = 0^{--}$, Phys. Rev. Lett. **129**, 102002 (2022).
[107] J.-M. Frère, An exotic path to glue states decay, in *Proceedings of the 23rd Hellenic School and Workshops on Elementary Particle Physics and Gravity* (2024), arXiv:2402.12211.
[108] B. Barsbay, K. Azizi, and H. Sundu, Light quarkonium hybrid mesons, Phys. Rev. D **109**, 094034 (2024).
[109] H.-X. Chen, Z.-X. Cai, P.-Z. Huang, and S.-L. Zhu, Decay properties of the 1^{-+} hybrid state, Phys. Rev. D **83**, 014006 (2011).
[110] P.-Z. Huang, H.-X. Chen, and S.-L. Zhu, Strong decay patterns of the 1^{-+} exotic hybrid mesons, Phys. Rev. D **83**, 014021 (2011).
[111] H.-X. Chen, N. Su, and S.-L. Zhu, QCD axial anomaly enhances the $\eta\eta'$ decay of the hybrid candidate $\eta_1(1855)$, Chin. Phys. Lett. **39**, 051201 (2022).

[112] A. A. Ovchinnikov and A. A. Pivovarov, QCD sum rule calculation of the quark gluon condensate, Sov. J. Nucl. Phys. **48**, 721 (1988).
[113] K.-C. Yang, W. Y. P. Hwang, E. M. Henley, and L. S. Kisslinger, QCD sum rules and neutron-proton mass difference, Phys. Rev. D **47**, 3001 (1993).
[114] J. R. Ellis, E. Gardi, M. Karliner, and M. A. Samuel, Renormalization-scheme dependence of Padé summation in QCD, Phys. Rev. D **54**, 6986 (1996).
[115] B. L. Ioffe and K. N. Zyablyuk, Gluon condensate in charmonium sum rules with three-loop corrections, Eur. Phys. J. C **27**, 229 (2003).
[116] M. Jamin, Flavor-symmetry breaking of the quark condensate and chiral corrections to the Gell-Mann-Oakes-Renner relation, Phys. Lett. B **538**, 71 (2002).
[117] V. Gimenez, V. Lubicz, F. Mescia, V. Porretti, and J. Reyes, Operator product expansion and quark condensate from lattice QCD in coordinate space, Eur. Phys. J. C **41**, 535 (2005).
[118] S. Narison, Gluon condensates and precise $\bar{m}_{c,b}$ from QCD-moments and their ratios to order α_s^3 and $\langle G^4 \rangle$, Phys. Lett. B **706**, 412 (2012).
[119] S. Narison, QCD parameter correlations from heavy quarkonia, Int. J. Mod. Phys. A **33**, 1850045 (2018); **33**, 1892004(A) (2018).
[120] R. D. Matheus, F. S. Navarra, M. Nielsen, and R. Rodrigues da Silva, Do the QCD sum rules support four-quark states?, Phys. Rev. D **76**, 056005 (2007).
[121] L. J. Reinders, H. Rubinstein, and S. Yazaki, Hadron properties from QCD sum rules, Phys. Rep. **127**, 1 (1985).
[122] S.-l. Zhu, W. Y. P. Hwang, and Z.-s. Yang, Electromagnetic decay of vector mesons as derived from QCD sum rules, Phys. Lett. B **420**, 8 (1998).
[123] H. Leutwyler, On the $1N-$ expansion in chiral perturbation theory, Nucl. Phys. B, Proc. Suppl. **64**, 223 (1998).
[124] R. Kaiser and H. Leutwyler, Pseudoscalar decay constants at large N_c, in *Proceedings of the Workshop on Methods of Nonperturbative Quantum Field Theory* (1998), pp. 15–29, arXiv:hep-ph/9806336.
[125] R. Escribano and J.-M. Frere, Study of the $\eta - \eta'$ system in the two mixing angle scheme, J. High Energy Phys. 06 (2005) 029.
[126] R. Escribano, P. Masjuan, and P. Sanchez-Puertas, The η transition form factor from space- and time-like experimental data, Eur. Phys. J. C **75**, 414 (2015).
[127] R. Escribano, S. Gonzàlez-Solís, P. Masjuan, and P. Sanchez-Puertas, η' transition form factor from space- and timelike experimental data, Phys. Rev. D **94**, 054033 (2016).
[128] J. Schechter, A. Subbaraman, and H. Weigel, Effective hadron dynamics: From meson masses to the proton spin puzzle, Phys. Rev. D **48**, 339 (1993).
[129] A. V. Kiselev and V. A. Petrov, Two schemes of $\eta - \eta'$ mixing, Z. Phys. C **58**, 595 (1993).
[130] P. Herrera-Siklody, J. I. Latorre, P. Pascual, and J. Taron, $\eta - \eta'$ mixing from $\mathrm{U}(3)_L \otimes \mathrm{U}(3)_R$ chiral perturbation theory, Phys. Lett. B **419**, 326 (1998).
[131] S. D. Bass and P. Moskal, η' and η mesons with connection to anomalous glue, Rev. Mod. Phys. **91**, 015003 (2019).
[132] G. S. Bali, V. Braun, S. Collins, A. Schäfer, and J. Simeth, Masses and decay constants of the η and η' mesons from lattice QCD, J. High Energy Phys. 08 (2021) 137.
[133] A. Ali, J. Chay, C. Greub, and P. Ko, Contribution of $b \to sgg$ through the QCD anomaly in exclusive decays $B^\pm \to (\eta', \eta)(K^\pm, K^{*\pm})$ and $B^0 \to (\eta', \eta)(K^0, K^{*0})$, Phys. Lett. B **424**, 161 (1998).
[134] T. Feldmann and P. Kroll, Flavor symmetry breaking and mixing effects in the $\eta\gamma$ and $\eta'\gamma$ transition form-factors, Eur. Phys. J. C **5**, 327 (1998).
[135] M. B. Voloshin and V. I. Zakharov, Measuring QCD anomalies in hadronic transitions between onium states, Phys. Rev. Lett. **45**, 688 (1980).
[136] R. Akhoury and J. M. Frere, η, η' mixing and anomalies, Phys. Lett. B **220**, 258 (1989).
[137] P. Castoldi and J. M. Frere, $\eta' \to \pi^+\pi^-\pi^0$: A key to understanding the $\eta - \eta'$ system, Z. Phys. C **40**, 283 (1988).
[138] K.-T. Chao, QCD axial anomaly and mixing of pseudoscalars, Nucl. Phys. **B317**, 597 (1989).
[139] P. Ball, J. M. Frere, and M. Tytgat, Phenomenological evidence for the gluon content of η and η', Phys. Lett. B **365**, 367 (1996).
[140] L. A. Griffiths, C. Michael, and P. E. L. Rakow, Mesons with excited glue, Phys. Lett. **129B**, 351 (1983). 881
[141] S. Perantonis and C. Michael, Static potentials and hybrid mesons from pure $SU(3)$ lattice gauge theory, Nucl. Phys. **B347**, 854 (1990).
[142] M. Foster and C. Michael, Hadrons with a heavy color-adjoint particle, Phys. Rev. D **59**, 094509 (1999).
[143] G. S. Bali and A. Pineda, QCD phenomenology of static sources and gluonic excitations at short distances, Phys. Rev. D **69**, 094001 (2004).
[144] J. J. Dudek, The lightest hybrid meson supermultiplet in QCD, Phys. Rev. D **84**, 074023 (2011).
[145] L. Liu, G. Moir, M. Peardon, S. M. Ryan, C. E. Thomas, P. Vilaseca, J. J. Dudek, R. G. Edwards, B. Joo, and D. G. Richards, Excited and exotic charmonium spectroscopy from lattice QCD, J. High Energy Phys. 07 (2012) 126.
[146] A. J. Woss, J. J. Dudek, R. G. Edwards, C. E. Thomas, and D. J. Wilson, Decays of an exotic 1^{-+} hybrid meson resonance in QCD, Phys. Rev. D **103**, 054502 (2021).